STUDY OF LOCAL SPECTRAL IRRADIANCE FOR THE APPLICATIONS OF ORGANIC PHOTOVOLTAIC

AARON HONG KAI JEAT

A project report submitted in partial fulfilment of the requirements for the award of the degree of Bachelor of Science (Hons.) Physics

Lee Kong Chian Faculty of Engineering and Science
Universiti Tunku Abdul Rahman

May 2016

DECLARATION

I hereby declare that this project report is based on my original work except for citations and quotations which have been duly acknowledged. I also declare that it has not been previously and concurrently submitted for any other degree or award at UTAR or other institutions.

Signature : _____

Name : Aaron Hong Kai Jeat

ID No. : 941211-05-5023

Date : _____

APPROVAL FOR SUBMISSION

I certify that this project report entitled **"STUDY OF LOCAL SPECTRAL IRRADIANCE FOR THE APPLICATIONS OF ORGANIC PHOTOVOLTAIC"** was prepared by **AARON HONG KAI JEAT** has met the required standard for submission in partial fulfilment of the requirements for the award of Bachelor of Science (Hons.) Physics at Universiti Tunku Abdul Rahman.

Approved by,

Signature : _____

Supervisor : Prof. Dr. Chong Kok Keong

Date : _____

The copyright of this report belongs to the author under the terms of the copyright Act 1987 as qualified by Intellectual Property Policy of University Tunku Abdul Rahman. Due acknowledgement shall always be made of the use of any material contained in, or derived from, this report.

© 2016, Aaron Hong Kai Jeat. All right reserved.

ACKNOWLEDGEMENTS

I would like to thank everyone who had contributed to the successful completion of this project. I would like to express my gratitude to my research supervisor, Prof. Dr. Chong Kok Keong for his invaluable advice, guidance and his enormous patience throughout the development of the research.

In addition, I would also like to express my gratitude to my loving parents and friends who had helped, supported and given me encouragement in spite of all the time this project took me away from them.

STUDY OF LOCAL SPECTRAL IRRADIANCE FOR THE APPLICATIONS OF ORGANIC PHOTOVOLTAIC

ABSTRACT

The performance of organic photovoltaic devices is greatly dependent on the local spectral irradiances, which is different attributed to spatial and atmospheric variations. In this project, the local spectral irradiances have been collected from January to July 2016 and all the data can be separated into three categories for organic solar cell performance analyses. The three categories of spectral irradiances are local direct spectral irradiance, local diffuse spectral irradiance, and the local total average spectral irradiance. The on-site measurements have shown that the peak intensities of the spectral irradiances are at the ranges of 550 – 600 nm, 500 – 550 nm, and 550 – 600 nm for local direct spectral irradiance, local diffuse spectral irradiance, and the local total average spectral irradiance respectively, while the peak intensity of the standard AM 1.5G reference is calculated at 450 – 500 nm. The red-shifted of local spectral irradiances were proved to grant better power conversion efficiency for the organic solar cells, as compared to the illumination of AM 1.5G spectrum. Among the studied organic materials, [PTB7:$PC_{60}BM$] shows the highest power conversion efficiency of 6.90% under local total average spectral irradiance, with an improvement of 10.10% with respect to illumination under AM 1.5G spectrum. The distribution of local average photon energy was studied to offer an alternative suggestion in organic solar cells bandgap designations for its use in the ASEAN region.

TABLE OF CONTENTS

DECLARATION **ii**
APPROVAL FOR SUBMISSION **iii**
ACKNOWLEDGEMENTS **v**
ABSTRACT **vi**
TABLE OF CONTENTS **vii**
LIST OF TABLES **ix**
LIST OF FIGURES **xi**
LIST OF SYMBOLS / ABBREVIATIONS **xv**
LIST OF APPENDICES **xvii**

CHAPTER

1 INTRODUCTION **1**
1.1 Research background 1
1.2 Research aims and objectives 2

2 LITERATURE REVIEW **4**
2.1 Weather conditions in Kajang, Malaysia 4
2.2 Local spectral irradiances in Kajang, Malaysia 5
2.3 Comparison of average photon energy measured in ASEAN region 6
2.4 The future of organic solar cells 7
2.5 Photovoltaics' data of various organic materials under AM 1.5G illumination 10

3 THEORY AND METHODOLOGY **11**
3.1 Integrated Spectral Irradiance 11
3.2 Average photon energy of local spectral irradiances 11
3.3 External quantum efficiency and device responsivity 12

3.4 Photovoltaics' data of organic solar cells 13
3.5 Air mass, relative humidity, and Naan & Riordan Considerations 14
3.6 Spectral irradiances collection uses AVANTES spectrometer 15
3.7 Simulations and calculations by Matrix Laboratory 16

4 RESULTS AND DISCUSSIONS 18
4.1 Local annual spectral irradiances versus reference standard AM 1.5G 18
4.2 Organic materials' performance under illumination of standard reference spectrum AM 1.5G 22
4.3 Organic materials' performance under illumination of various local spectral irradiances 26
4.3.1 Local direct spectral irradiance illumination 27
4.3.2 Local diffuse spectral irradiance illumination 30
4.3.3 Local total average spectral irradiance illumination 33
4.3.4 Summary of the organic materials' performance under different spectral irradiance illumination conditions 36
4.4 Local average photon energy distribution 38
4.5 Probability of getting direct spectral irradiance during daytime 40

5 CONCLUSIONS AND RECOMMENDATIONS 42

REFERENCES 44

APPENDICES 47

LIST OF TABLES

TABLE	TITLE	PAGE
2.1:	Parameters of Various Organic Materials under AM 1.5G Illumination	10
4.1:	Weightage of each specific wavelength range of various spectral irradiance (300 nm – 1100 nm)	21
4.2:	Various organic solar materials' photovoltaic data under the illumination of AM 1.5G (Improvement of PCE compared to published AM 1.5G)	25
4.3:	Various organic materials' photovoltaic data under the illumination of local direct spectral irradiance (Improvement of PCE compared to AM 1.5G)	29
4.4:	Various organic materials' photovoltaic data under the illumination of local diffuse spectral irradiance (Improvement of PCE compared to AM 1.5G)	32
4.5:	Various organic materials' photovoltaic data under the illumination of local diffuse spectral irradiance (Improvement of PCE was done with respect to local direct spectral irradiance PCE (L. Direct PCE)	32

4.6: Various organic solar cells' photovoltaic data under the illumination of local total average spectral irradiance (Improvement of PCE compared to AM 1.5G) 36

4.7: Power conversion efficiency (%) of each of the organic materials subjected to different spectral irradiance illuminations 37

4.8: Power conversion efficiency (%) improvement of each of the organic materials with respect to AM 1.5G Spectrum 37

LIST OF FIGURES

FIGURE	TITLE	PAGE
2.1:	Average photon energy measured under Thailand climatic conditions (taken from (Sirisamphanwong, 2011))	7
2.2:	Conventional structure of organic solar cells with bottom-illumination (taken from (Lim, 2012))	8
2.3:	Inverted structure of organic solar cells with bottom-illumination (taken from (Lim, 2012))	9
3.1:	Processing steps of spectral irradiance collection by the AVANTES spectrometer	16
3.2:	The main part of the MATLAB's coding that used to calculate the values of *ISI* and *APE*	17
4.1:	Local annual direct spectral irradiance at each hour (8.00 am - 6.00 pm) versus wavelength (the middle period for each hour, for example 830 denotes as 0800 – 0859 for convenience of results presentation)	18
4.2:	Local diffuse spectral irradiance at each hour (8.00 am - 6.00 pm) versus wavelength (the middle period for each hour, for example 830 denotes as 0800 – 0859 for convenience of results presentation)	20

4.3: Local spectral irradiance collected in total average (blue line), local direct (green line), and local diffuse (red line), by comparing to AM 1.5G (yellow-red marker) 20

4.4: External Quantum Efficiency (*EQE*) of organic materials under the illumination of AM 1.5G spectrum (The yellow-red marker is AM 1.5G spectrum, while the coloured smooth lines are device *QE*) 23

4.5: Responsivity of organic materials under the illumination of AM 1.5G spectrum (The yellow-red marker is AM 1.5G spectrum, while the coloured smooth lines are device responsivity) 24

4.6: Current density (in the function of wavelength) of each of the organic materials under illumination of AM 1.5G (The yellow-red marker is AM 1.5G spectrum, while the coloured smooth lines are device current density) 24

4.7: External Quantum Efficiency (EQE) of organic materials under the illumination of local direct spectral irradiance (green line with solid symbol denotes the local direct spectral irradiance, while the coloured smooth lines are device QE) 27

4.8: Responsivity of organic materials under the illumination of local direct spectral irradiance (green line with solid symbol denotes the local direct spectral irradiance, while the coloured smooth lines are device responsivity) 28

4.9: Current density (in the function of Wavelength) of each of the organic materials under illumination of local direct spectral irradiance (green line with solid symbol denotes the local direct spectral irradiance, while the coloured smooth lines are device current density) 28

4.10: External Quantum Efficiency (EQE) of organic materials under the illumination of local diffuse spectral irradiance (red line with solid symbol denotes the local diffuse spectral irradiance, while the coloured smooth lines are device QE) 30

4.11: Responsivity of organic materials under the illumination of local diffuse spectral irradiance (red line with solid symbol denotes the local diffuse spectral irradiance, while the coloured smooth lines are device responsivity) 31

4.12: Current density (in the function of wavelength) of each of the organic materials under illumination of local diffuse spectral irradiance (red line with solid symbol denotes the local diffuse spectral irradiance, while the coloured smooth lines are device current density) 31

4.13: External Quantum Efficiency (EQE) of organic materials under the illumination of local total average spectral irradiance (light-blue line with solid symbol denotes the local total average spectral irradiance, while the coloured smooth lines are device QE) 34

4.14: Responsivity of organic materials under the illumination of local total average spectral irradiance (light-blue line with solid symbol denotes the local total average spectral irradiance, while the coloured smooth lines are device responsivity) 35

4.15: Current density (in the function of Wavelength) of each of the organic materials under illumination of local total average spectral irradiance (light-blue line with solid symbol denotes the local total average spectral irradiance, while the coloured smooth lines are device current density) 35

4.16: Distribution of average photon energy (APE) for local direct and local diffuse spectral irradiances (green bars indicate local direct spectrum APEs; red bars indicate local diffuse spectrum APEs) 39

4.17: Distribution of average photon energy (APE) under local total average spectral irradiance illumination 39

4.18: Probability of having direct sunlight throughout the day on the site at Universiti Tunku Abdul Rahman (UTAR), Kajang, Malaysia (the middle period for each hour, for example 830 denotes as 0800 – 0859 for convenience of results presentation) 41

LIST OF SYMBOLS / ABBREVIATIONS

ISI	integrated spectral irradiance, W/m^2
$E(\lambda)$	spectral irradiance, W/m^2 nm
APE	average photon energy, eV
$\phi(\lambda)$	spectral photon flux density, photons/m^2 nm
λ	wavelength, nm
h	Planck's constant, 6.626×10^{-34} J s
c	speed of light, 2.998×10^{8} m/s
q	electric charge, 1.602×10^{-19} C
η_{EQE}	external quantum efficiency
I_{ph}	photo-generated current/collectable electrons, A
P_o	incident optical power, W
R	responsivity, A/W
J_{SC}	short circuit current density, mA/cm^2
V_{OC}	open circuit voltage, V
FF	fill factor (%)
PCE	power conversion efficiency (%)
R_p	parallel resistance of the device, Ω
R_s	series resistance of the device, Ω
n	ideality factor
k_B	Boltzmann's constant, 1.381×10^{-23} J/K
T	device operating temperature, K
J_s	reverse saturation current density, mA/cm^2
ASEAN	Association of Southeast Asian Nations
OSCs	organic solar cells
AM	air mass

AM 1.5G	AM 1.5 global spectrum
ASTM	American Society for Testing and Materials
USA	United State of America
EHPs	electron-hole pairs
ITO	indium tin oxide
Device QE	device quantum efficiency
J	current density
V	voltage
MATLAB	Matrix Laboratory

LIST OF APPENDICES

APPENDIX	TITLE	PAGE
Table A.1	Weightage for Specific Wavelength Range for each Hour under the Illumination of Local Direct Spectral Irradiance (the cells' values that have weightage more than 0.80 will be yellow-coloured, which is used to compare the shift of the spectral irradiance of each hour)	47
Table A.2:	Weightage for Specific Wavelength Range for each Hour under the Illumination of Local Direct Spectral Irradiance (the cells' values that have weightage more than 0.80 will be yellow-coloured, which is used to compare the shift of the spectral irradiance of each hour)	48
Figure A 1:	Comprehensive method for analysing the *PCE* of *OSCs* under different spectral irradiances considering both photonic and electrical characteristics (page 1)	49
Figure A 2:	Comprehensive method for analysing the *PCE* of *OSCs* under different spectral irradiances considering both photonic and electrical characteristics (page 2)	50

Figure A 3: Comprehensive method for analysing the *PCE* of *OSCs* under different spectral irradiances considering both photonic and electrical characteristics (page 3) 51

Figure A 4: Comprehensive method for analysing the *PCE* of *OSCs* under different spectral irradiances considering both photonic and electrical characteristics (page 4) 52

Figure A 5: Comprehensive method for analysing the *PCE* of *OSCs* under different spectral irradiances considering both photonic and electrical characteristics (page 5) 53

Figure A 6: Comprehensive method for analysing the *PCE* of *OSCs* under different spectral irradiances considering both photonic and electrical characteristics (page 6) 54

Figure A 7: Comprehensive method for analysing the *PCE* of *OSCs* under different spectral irradiances considering both photonic and electrical characteristics (page 7) 55

Figure A 8: Comprehensive method for analysing the *PCE* of *OSCs* under different spectral irradiances considering both photonic and electrical characteristics (page 8) 56

CHAPTER 1

INTRODUCTION

1.1 Research background

Spectral irradiance (solar spectrum) is one of the crucial factors that affect the performance of photovoltaic devices, such as solar cells. Rotation of the Earth allows majority parts of the world able to receive enough sunlight that enables it to be harvested by the solar panels to generate electricity for the society. In order to generalize the spectral irradiance received by every part of the world, a reference standard spectrum, which is known as AM 1.5G was calculated. Majority of the solar manufacturers in the world are currently designing and producing photovoltaic devices based on AM 1.5G spectrum. However, due to latitude of each country is different with respect to one another, the spectral irradiance received by each country will ultimately have deviations with respect to AM 1.5G. The realization of this issue that will affect the solar cells' performance had caught the attention of the international solar community. Following from that, intensive researches on the local spectral irradiance on each geographical area have been carried out. The research on local spectral irradiance, especially in ASEAN region is still not widely carried out. Furthermore determination on the tailoring of bandgap of solar cells based on the local spectral irradiance is even less. Hence, the main topic for this project will be tailoring the solar cells based on the local spectral irradiances in the ASEAN region to obtain best power conversion efficiency.

The solar cell types that have chosen to study for this project is organic solar cells (*OSCs*). In the current solar industry, the dominating material for the

manufacturing solar cells is silicon (*Si*) based solar cells, which having up to 85% of market share (Wang, 2016). Although Si-based solar cells is a promising green-technology, the applications of it is not widespread due to high production cost for its critical manufacturing processing. As for the *OSCs*, the production cost can be effectively lowered due to the introduction of low cost roll-to-roll technique (Tanenbaum, 2011) for its large area of fabrication. The other advantages, including its flexibility and dynamics in tailoring molecular properties (Institute of Science in Society, 2006) are attracting international research groups to study on its potential applications in order to utilize the advantages of *OSCs*.

The project was started by investigating of local spectral irradiances in Malaysia through data collection that conducted in Universiti Tunku Abdul Rahman (UTAR), Jalan Sungai Long, Bandar Sungai Long, 43000 Kajang, Selangor, Malaysia. The latitude and longitude of UTAR are 3.0408˚N and 101.7942˚E respectively. The data collection has taken place for 7 months (January 2016 to July 2016), from 8.00 am to 6.00 pm for every data collection day. The main device that used was AVANTES spectrometers, which comprised of AvaSpec-2048-USB2-RM (bandwidth: 200 – 1100 nm) and AvaSpec-NIR256-1.7-RM (bandwidth: 1000 – 1750 nm). The second part of this project would be studying the performance of the organic materials' groups theoretically through journal papers that were available. The locally collected spectral irradiance data were then fit into the calculations of each of the organic materials to obtain the power conversion efficiency (*PCE*) respectively.

1.2 Research aims and objectives

The aim of this project is to tailor the bandgap of organic materials to the local spectral irradiances in the ASEAN region in order to obtain best power conversion efficiency. The objectives for this project are described as follows:

1. To verify the differences of local spectral irradiances with respect to the standard reference AM 1.5G through spectrum analysis

2. To determine the performance of the *OSCs* based on the local spectral irradiances, including local direct spectral irradiance (clear sky), local diffuse spectral irradiance (cloudy condition), and also total average of local spectral irradiance
3. To select the best available organic materials for the *OSCs* designation in the ASEAN region

CHAPTER 2

LITERATURE REVIEW

2.1 Weather conditions in Kajang, Malaysia

Kajang is a city that situated in the west of the Peninsular Malaysia, which is roughly about 23 km away from the Malaysia's national capital, Kuala Lumpur. Due to its unique location, which is near to the Earth's Equator, temperature in Malaysia is nearly uniform throughout the year (Malaysian Meteorological Department, 2016). The temperature recorded from June 1, 2015 until July 2016 is ranging from 24 ˚C to 33˚C (Underground, 2016). Every year, Malaysia will expose to two main seasonal variations, which are the northeast monsoon season and southwest monsoon season. During these 2 seasons, including the periods of the interchange of seasons, the rainfall distributions will be varied accordingly. For instance in Peninsular Malaysia, the rainfall (small intensity) was recorded to have 70% and more than 80% occurrence during the northeast monsoon and southwest monsoon seasons respectively (Varikoden, 2011). This in turns will affect the local spectral irradiances, and also its exposure hours. The average exposure hours in the direct sunlight in Malaysia was recorded to be 6 hours (Malaysian Meteorological Department, 2016), and the duration of exposure hours will be varied according to the geographical variations in Malaysia. Due to the local average high temperature, this normally leads to high evaporation of water during the daytime, which eventually increases the relative humidity level of the air in Malaysia in the range of 70% - 90% (McGinley, 2011).

2.2 Local spectral irradiances in Kajang, Malaysia

Local spectral irradiances play a vital role in the performance of solar cells' technologies, as it depends on the local weather conditions. For each of the materials used for manufacturing of photovoltaic devices, the corresponding performance is limited by its spectral response width, whereby the solar cells only able to harvest a certain wavelength range of light energy and convert it into useful electrical current. There are several factors that may contribute to the deviation of the local spectral irradiance from standard reference AM 1.5G, such as the path length through the atmosphere (Air Mass, *AM*), the amounts of water vapour in the atmosphere, aerosol content (Mambrini, 2015), cloud coverage, solar zenith angle (S. Nann & C. Riordan, 1991). All these factors vary according to geographical locations, and also the local weather conditions.

Due to the presence of many factors that making a significant impact to the local spectral irradiances, the American Society for Testing and Materials (ASTM) have published three international standard spectra for basic theoretical calculations and as the basis for majority solar cells' designations (Newport Corp., n.d.). The 3 spectra including AM 0, AM 1.5 Direct (AM 1.5D), and AM 1.5 Global (AM 1.5G). Considering the installation of most of the solar panels on the ground, the standard reference AM 1.5G is adopted for most of the materials' selection and solar cells designations. However, AM 1.5G is obtained based on the average weather conditions of the 48 contiguous states in the United States of America (USA), by taking solar zenith angle and tilted surface angle at 48˚ and 37˚, respectively (Green Rhino Energy, n.d.). Moreover, the local albedo, which also known as surface reflectivity (S. Nann & C. Riordan, 1991) and the turbidity (cloudiness) were set to be 0.3 and 0.29, respectively, under an ambient temperature of 20˚C (U.S. Standard Atmosphere, 1976). All these conditions are harsh to be satisfied by all the countries across the globe (except in USA) due to variations of local spatial and atmospheric conditions. Hence, a study of the local spectral irradiances on certain region ("ASEAN region" for this project) is required.

2.3 Comparison of average photon energy measured in ASEAN region

Average photon energy (*APE*) is another foremost parameter that affects the performance of photovoltaic devices. Some studies [(C. Cornaro & A. Andreotti, 2013); (Sirisamphanwong, 2014); (Nofuentes, 2014)] have shown the linear dependency between the performance of certain solar cells to the *APE* values, especially in the solar cells (*OSCs*) that having a narrow spectral response width. The basic working methodology of solar cell starts with capturing the energy from the incoming photons, generating electron-hole pairs (*EHPs*). Then, *EHPs* would be separated at the interface of the active layers due to present of the internal electric field that generated from the potential difference between the bandgap of the donor/acceptor materials. For narrow bandgap materials, they will only respond to a narrow wavelength range of photons. Owing to this reason, the incoming photons with appropriate *APE* values will be considered "useful" to the organic materials. The photons that have relatively high *APE* values than the materials' bandgap will be absorbed near the surface of the photovoltaic device due to surface recombination (Kasap, 2001); while photons that have lower *APE* values than the materials will be wasted, as it is not large enough to photo-generate *EHPs*. This eventually will affect the open-circuit voltage (V_{OC}) of *OSCs* (Brus, 2015) that lead to low power conversion efficiency. Hence an optimum bandgap of organic materials should be considered for the *OSCs*' designations by examining the distribution of local measured *APE* values.

Figure 2.1 (Sirisamphanwong, 2011) shows the annual *APE* values obtained from Naresuan University in Thailand. The spectral range that used for the analysis by them is 350 nm – 1050 nm, which covered up most of the solar cells' spectral response region. The integrated spectral irradiance (*ISI*) measured by them is at 420 – 710 W/m^2. 50% of the *APE* values that measured by C. Sirisamphanwong's groups are higher than the standard reference AM 1.5G, which is at 1.88 eV. Due to the presence of seasonal variations in Thailand, the measured *APE* values for summer, winter, and raining seasons were recorded at 1.92 eV, 1.84 eV, and 1.90 eV respectively. These *APE* values were calculated through the annual local spectral irradiances.

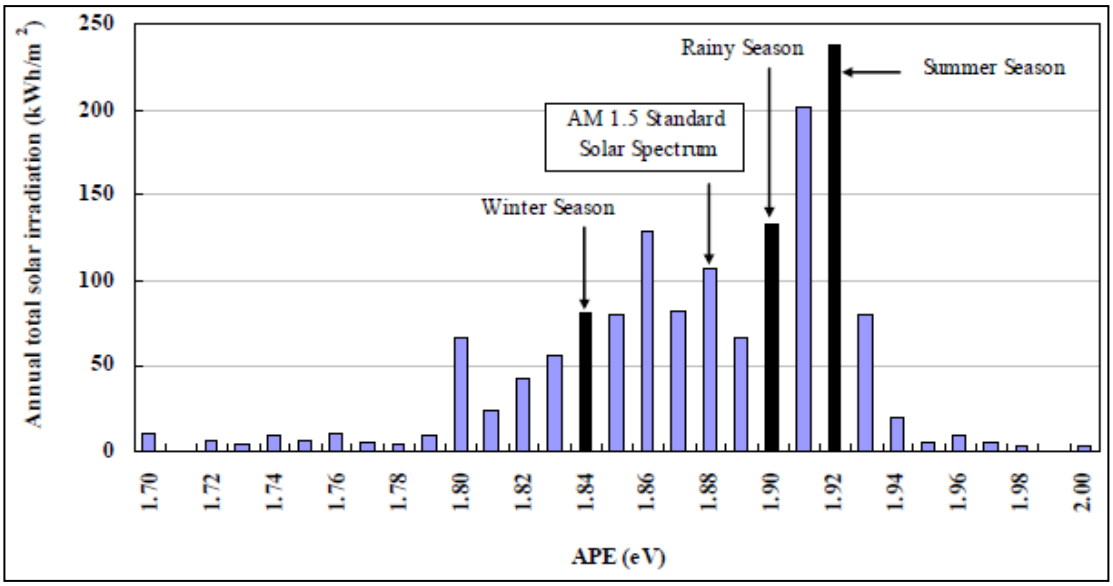

Figure 2.1: Average photon energy measured under Thailand climatic conditions (taken from (Sirisamphanwong, 2011))

2.4 The future of organic solar cells

In the last few decades, under the laboratory conditions, it is possible to produce monocrystalline silicon (*Si*) solar cell with the power conversion efficiency (*PCE*) that able to achieve up to 25% (Shwartz, 2015). Although this efficiency is considerably high, but it suffers from high production cost due to complex fabrication process (Wang, 2016). For this reason, many household consumers have opted for a more affordable type of solar panel, which is the polycrystalline silicon-based, however the *PCE* to date is reported around 20% (Mat-Desa, 2016). Another challenge that faced by silicon-based solar cells is, based on the Shockley-Queisser limit prediction, *PCE* of *Si*-based solar cell is predicted to bottle-necked at 30% (Shockley and Queisser , 1961).

The high cost involved in manufacturing monocrystalline *Si*-based solar cells and also its efficiency is reaching near to the theoretical limit have urged the international solar research community to search for new alternative materials. One of the most well-known alternative material types in the current studies is the organic materials. Organic materials are frequently possessed high absorption coefficient,

which up to ~ 10^5 cm^{-1} (Savenije, 2014). Other advantages that able to be offered by *OSCs* are aforementioned in Section 1.1. However, the main drawback of the current *OSCs* is its low *PCE* values, as compare to *Si*-based solar cell, which partly due to the narrow absorption band. For instance, the absorption band of majority organic materials is within 300 nm – 900 nm [(Liu, 2014); (Morinaka, 2013); (Fan, 2014)]. The highest recorded *PCE* to date under laboratory condition is 13.2%, which achieved by Heliatek R&D team in Germany. In addition to this, there are several factors that lead to higher rate of degradation in *OSCs*, these include majority of the organic materials are not chemically inert to the oxygen and water molecules (Madsen, n.d.), and self-etching of indium tin oxide (*ITO*) electrode under direct illumination with acidic *PEDOT:PSS* layer (Wang, 2016).

In order to increase the *PCE* of the *OSCs*, the study of local spectral irradiances was recommended to find the deviation of the peak with respect to AM 1.5G (Chong, 2016); to prolong the lifetime of the *OSCs*, many alternative designs have come up with, such as the inverted structure of *OSCs*. The designs of the OSCs' conventional structure and inverted structure are illustrated in Figure 2.2 and Figure 2.3 respectively (Lim, 2012). The polarity of the charged generation is reversed in inverted *OSCs* with respect to the conventional structure.

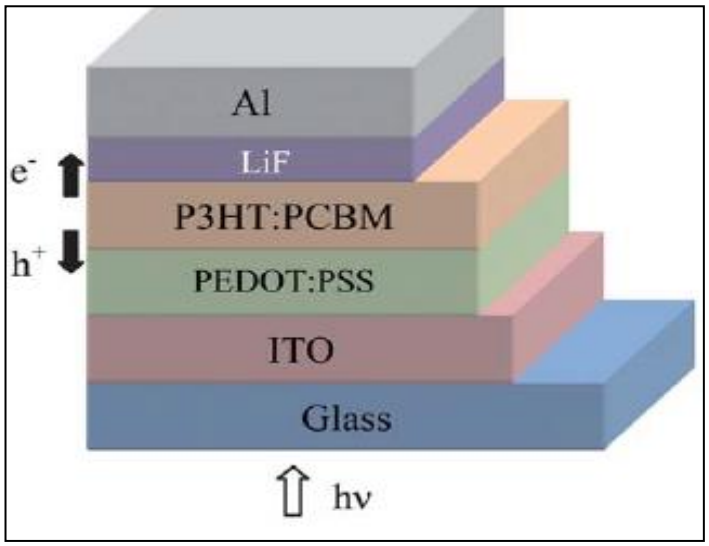

Figure 2.2: Conventional structure of organic solar cells with bottom-illumination (taken from (Lim, 2012))

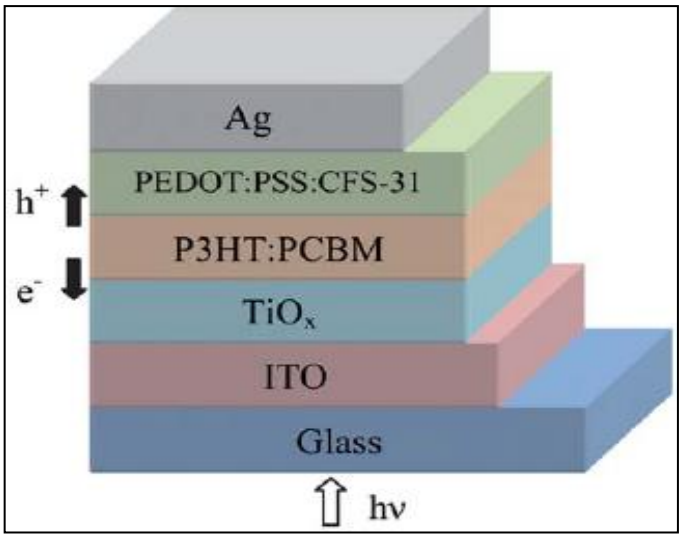

Figure 2.3: Inverted structure of organic solar cells with bottom-illumination (taken from (Lim, 2012))

The conventional *OSC* stack (Figure 2.2) is [ITO / PEDOT:PSS / P3HT:PCBM / LiF / Al], which can be further described as follows:

- *ITO* = anode
- *PEDOT:PSS* = hole transport layer (HTL)
- *P3HT:PCBM* = active layer
- *LiF* (*lithium fluoride*) = electron injection layer (EIL)
- *Al* (*aluminium*) = cathode

The inverted *OSC* stack consists of (Figure 2.3) [ITO / TiO_x / P3HT:PCBM / PEDOT:PSS:CFS-31 / Ag], which can be further described as follow:

- *ITO* = cathode
- *TiO_x* = electron-transporting layer (ETL)
- *P3HT:PCBM* = active layer
- *PEDOT:PSS:CFS-31* = hole transport layer (HTL)
- *Ag (silver)* = anode

2.5 Photovoltaics' data of various organic materials under AM 1.5G illumination

For analysing the *PCE* of different organic materials (only in the active layer) under various local spectral irradiances, there are few critical parameters we need to consider such as materials' group (electron donor/ electron acceptor), open-circuit voltage (V_{OC}), short circuit current density (J_{SC}), fill factor (*FF*), and the *PCE*. In addition to these, the device quantum efficiency (*QE*) is also another important parameter to consider in the calculations due to present of different spectral response region for each organic material. Those values are able to obtain from the published results from each experimental group. The organic materials' groups that were studied under this project are as follows:

1. PTBFTDTBT:$PC_{71}BM$ (Fan, 2014)
2. PTB7:$PC_{60}BM$ (Morinaka, 2013)
3. P3HT:$PC_{60}BM$ (Morinaka, 2013)
4. PCPDTBT:$PC_{71}BM$ (R. Lin, 2014)
5. PCDTBT:$PC_{70}BM$ (Liu, 2014)

The reference values for V_{OC}, J_{SC}, *FF*, and also *PCE* under the AM 1.5G illumination for the mentioned organic materials groups are shown in Table 2.1.

Table 2.1: Parameters of Various Organic Materials under AM 1.5G Illumination

Organic Materials	**V_{OC} (V)**	**J_{SC} (mA/cm^2)**	**FF (%)**	**PCE (%)**
PTBFTDTBT:$PC_{71}BM$	0.80	14.21	51.4	5.84
PTB7:$PC_{60}BM$	0.76	13.28	62.0	6.24
P3HT:$PC_{60}BM$	0.61	7.84	69.0	3.27
PCPDTBT:$PC_{71}BM$	0.63	11.10	42.2	2.93
PCDTBT:$PC_{70}BM$	0.88	10.80	49.0	4.66

CHAPTER 3

THEORY AND METHODOLOGY

3.1 Integrated Spectral Irradiance

Integrated spectral irradiance (*ISI*) is the summation of whole spectrum wavelengths' intensities by integrating the spectral irradiance in the function of wavelength, as shown in Equation (1).

$$ISI = \int E(\lambda) d\lambda \tag{1}$$

where $E(\lambda)$ is the spectral irradiance (Watt per meter-squared per wavelength (nm)), $d(\lambda)$ is the step size between the wavelength to its adjacent (both of them are obtained from the AVANTES spectrometers in this project). The lower and upper integration limits for the wavelength in this project were set at 280 nm and 1750 nm respectively.

3.2 Average photon energy of local spectral irradiances

Average photon energy (*APE*) is the calculation of total energy divided by total incoming photons from the Sun, as shown in Equation (2). *APE* is a parameter that often used to characterize the pattern of the local spectral irradiance [(Nofuentes, 2014); (Norton, 2015)]. Thus, for a higher *APE* values with respect to others, it means the respective spectral irradiance is more blue-shifted in comparing with others. This parameter in fact, having significant impact to narrow spectral response width solar

cells, such as organic solar cells (*OSCs*) and amorphous silicon solar cells, as aforementioned in Section 2.3.

$$APE = \frac{\int E(\lambda)d\lambda}{q \bullet \int \phi(\lambda)d\lambda} \tag{2}$$

The $\phi(\lambda)$ is the spectral photon flux density (photons per meter-squared per second), λ is the wavelength of the incoming photons, $E(\lambda)$ is the spectral irradiance, h is the Planck's constant, and c is the speed of light.

3.3 External quantum efficiency and device responsivity

External quantum efficiency (*EQE*) or device quantum efficiency (*QE*) is defined as the number of the free electron-hole-pairs (*EHPs*) that collected to the number of incident photons, as shown in Equation (3). *EQE* of each of the device is different due to different active layer's materials were used to harvest photon energy.

$$\eta_{EQE} = \frac{I_{ph}/q}{P_o/h\nu} = \frac{I_{ph}}{P_o}\left(\frac{hc}{q\lambda}\right) \tag{3}$$

I_{ph}/q is refers as the number of collectable electrons per second; while $P_o/h\upsilon$ is defines as the number of the incident photons per second. h is the Planck's constant, c is the speed of light, e is the electron's charge, and λ is the photon's wavelength. Device responsivity is a similar term to *EQE*, which is also used to characterize a photovoltaics' performance. It defines in terms of the ratio of photocurrent (I_{ph}) generated to the incident optical power (P_o), as shown in Equation (4).

$$R = \frac{I_{ph}}{P_o} \tag{4}$$

Device responsivity may also defines in terms of device *QE*, as shown in Equation (5). Now the device responsivity will depend on the device *QE* and also the incident photon's wavelength.

$$R = \eta_{EQE}\left(\frac{q\lambda}{hc}\right) \tag{5}$$

3.4 Photovoltaics' data of organic solar cells

Along with device *QE* and also device responsivity, the photovoltaics' data that including short circuit current density (J_{SC}), open circuit voltage (V_{OC}), fill factor (*FF*), and power conversion efficiency (*PCE*) will be used to characterize the performance of an organic solar cell. The relationship between current density (*J*) and voltage (*V*) of solar cells is generalized under Shockley's equation [(Chong, 2016); (Foster, 2013)], which is shown in Equation (6).

$$J = \frac{R_p}{R_s + R_p}\left\{J_s\left[\exp\left(\frac{q(V - JR_S)}{nk_BT}\right) - 1\right] + \frac{V}{R_p}\right\} - J_{ph} \tag{6}$$

R_p is the parallel resistance, R_s is the series resistance, *n* is the ideality factor, k_B is the Boltzmann's constant, *e* is electrical charge, *T* is the device operating temperature, and J_s is the reverse saturation current density (Kasap, 2001). By making the assumptions that, the organic solar cells having minimal leakage current ($R_p \rightarrow \infty$), low R_s values, and ($J_{ph} >> J_s$), the J_{SC} and the V_{OC} will be defined as Equation (7) and Equation (8) respectively [(Chong, 2016); (Würfel, 2015); (Guechi, 2013)].

$$J_{SC} = -J_{ph} \tag{7}$$

$$V_{OC} \approx \frac{nk_BT}{q}\ln\left(\frac{J_{SC}}{J_s}\right) \tag{8}$$

The fill factor and the power conversion efficiency can be calculated as shown in Equation (9) and Equation (10) respectively (Kasap, 2001).

$$FF = \frac{J_{\max} V_{\max}}{J_{SC} V_{OC}} \tag{9}$$

$$PCE = FF \times \frac{J_{SC} V_{OC}}{P_o / A} \tag{10}$$

J_{max} and V_{max} are the maximum possible current density and voltage that can be delivered by the *OSCs*, while the P_o/A is the incident optical power per unit area received by the *OSCs*.

3.5 Air mass, relative humidity, and Naan & Riordan Considerations

Air mass (*AM*) is the ratio of actual sunlight's travel distance from the atmosphere to the Earth's surface with respect its shortest path it can take to reach the surface (Kasap, 2001). The shortest distance where the sunlight travels occur is when the position of the Sun is directly above the specific location on the Earth. Variation of *AM* values will affect the intensity of local spectral irradiances as it affects by the absorption and scattering effects that present in the particular location's atmosphere. For high *AM* value, the Sun's beam takes longer path and will subjected to more absorption and scattering effect, which leads to low intensity in the local spectrum (Guechi, 2013).

Relative humidity is the ratio of the actual water vapour density to the saturation water vapour density in the air at a particular temperature. The relative air humidity level in Malaysia was recorded in the range 70% - 90% (McGinley, 2011), and the local spectral irradiances is dependent on water vapour content in the local atmosphere (C. Cornaro & A. Andreotti, 2013). Generally the relative humidity in the morning is high when the temperature is low; while the relative humidity reaches its minimum when the temperature is the highest during noon hours (FAO Corp. Doc. Repository, n.d.). Hence, by comparing the spectral irradiances under local clear day condition throughout the day, during the morning or evening hours, the solar spectrums

appear to be red-shifted with respect to the solar spectrums during noon hours. By understanding this trend, the performance of the organic photovoltaic devices is then understood, where it performed better in the afternoon, than in the morning or evening hours, as J_{SC} and V_{OC} values of the *OSCs* are having linear dependency to the local spectral irradiances (Kazem, 2012).

Naan and Riordan's works are based on the effect of overcast condition to the local spectral irradiances received at the Earth's surface. Generally during cloudy or rainy days, the travelling path of the Sun's beam would be obstructed by cloud layer. Based on their studies, highly energetic photons are reported to have a higher transmission probability than the low energetic photons by 30%, during overcast conditions. Local diffuse spectral irradiance eventually shown to be blue-shifted (also known as bluish enhancement) with respect to local direct spectral irradiance, in terms of their relative peak intensities (S. Nann & C. Riordan, 1991).

3.6 Spectral irradiances collection uses AVANTES spectrometer

The collection of the spectral irradiances was conducted at Universiti Tunku Abdul Rahman (UTAR), by the spectrometer. The time of the data collection was set from 8.00 am to 6.00 pm, and the spectral width was set to be recorded at 200 nm to 1100 nm by the counter AvaSpec-2048-USB2-RM (near-ultra-violet region: visible region, NUV:VIS); while the spectral width between 1000 nm to 1750 nm was set to be recorded by the counter AvaSpec-NIR256-1.7-RM (visible region: near-infrared region, VIS:NIR). These 2 ranges of data were then merged into a single file. The data were collected at each 15 minutes interval.

Before beginning any data collection, it is necessary to remove any potential local background noise that might be recorded by the spectrometer. In order to differentiate the background noise and the spectral irradiance intensity, a dark cover-slid was made to cover the detector of the spectrometer. The detector was designed to capture any Sun's beam (photons) that falls onto it, and the results would be displayed on the computer screen. Upon the detector was covered up by the cover-slid, which in

perfect case no light intensity for the whole spectrum would be detected. However, during the on-site measurements, there are some light intensities at certain wavelength range may still detectable. This would be recognised as potential local background noise, and the spectrometer was set to remove it in order to ensure the accuracy of the collected data.

Figure 3.1 shows the steps in collecting the spectral irradiance data. A long metal strip was constructed on the platform to check for the presence of shadow. The detector was then tied up with the metal strip to ensure its alignment is parallel to the metal strip. For every 15 minutes, the sensor would be adjusted to point directly to the Sun, which would be double confirmed by the long metal strip by having no shadow appear on the platform. The spectrum data was then merged and saved by the AVANTES' software in a "spec" file, and then converted to Microsoft Excel file in the computer for further analysis.

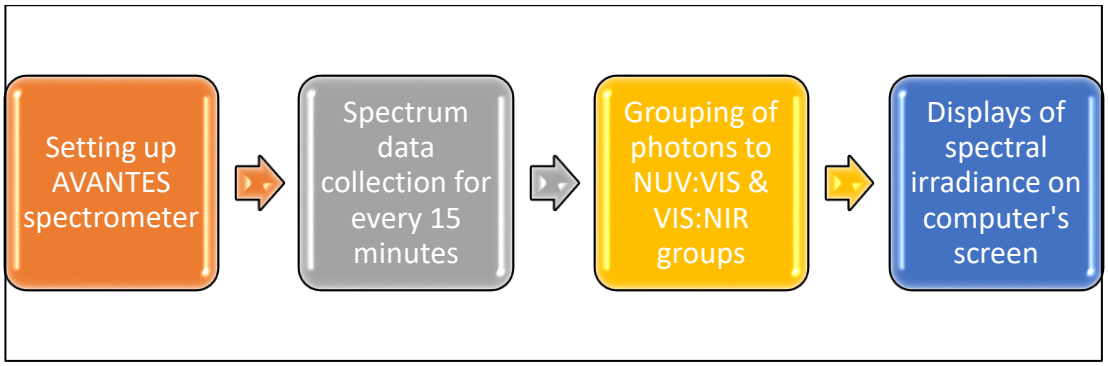

Figure 3.1: Processing steps of spectral irradiances collection by the AVANTES spectrometer

3.7 Simulations and calculations by Matrix Laboratory

Matrix Laboratory (MATLAB) is known for performing simulation, analysis, and calculation, based on a large primary data obtained from the experiment. In this project, the data of spectral irradiances that converted into Excel files would be computed by the MATLAB to perform simulations. A simple explanation of the MATLAB algorithm that used for this project would be done by using the language of pseudocode.

First, the declaration of all the variables and arrays were done. Then the initiation of certain variables, by pre-setting certain variable arrays to be zero before filling in any data. The wavelength range of the light source (which is the Sun) and the respective intensity for each wavelength was called into the MATLAB from the first Excel file. The calculations of the *ISI* and *APE* values would be done by using the Equations (1) and (2). The whole process would be repeated by calling in the next file, until all the data files that collected have been successfully inserted in. The corresponding graphs would then be displayed out for analysis or comparison purposes. A small part of the MATLAB code, which is the vital part of the *ISI* and *APE* calculations is shown in Figure 3.2.

```
for k=1:num_file;
  data{k}=xlsread(fullfile(folder,d(k).name));
  %Extraction of values
  colC(:,k)=data{k}(102:1822,1);%wavelength (nm),102:1822,263:1532
  colD(:,k)=data{k}(102:1822,2);%intensity (micro W/cm^2/nm),102:1822,263:1532
  colD(colD<0)=0;
  filename{k}=['',d(k).name];

  %Calculation
  C(:,k)=diff(colC(:,k)); %different in wavelength (nm)
  D(:,k)=0.5*(colD((1:end-1),k)+colD((2:end),k)); %average of the intensity (micro W/cm^2 nm)
  ISI(k,1)=sum(C(:,k).*D(:,k))/100; %(W/m^2)

  Total(k,1)=sum((C(:,k).*D(:,k))*10^(-2).*colC((2:end),k)*10^(-9));
  phi(k,1)=Total(k,1)/(6.626*10^(-34)*3*10^(8)); %photon flux
  APE_ans(k,1)=ISI(k,1)/(1.602*10^(-19)*phi(k,1)); %APE
end
```

Figure 3.2: The main part of the MATLAB's coding that used to calculate the values of *ISI* and *APE*

CHAPTER 4

RESULTS AND DISCUSSIONS

4.1 Local annual spectral irradiances versus reference standard AM 1.5G

The spectral irradiances' graphs that illustrated in this section was divided into 3 sections, which are local direct spectral irradiance for each hour, local diffuse spectral irradiance for each hour, and local annual average spectral irradiances. The obtained results were then compared to AM 1.5G to observe the deviation.

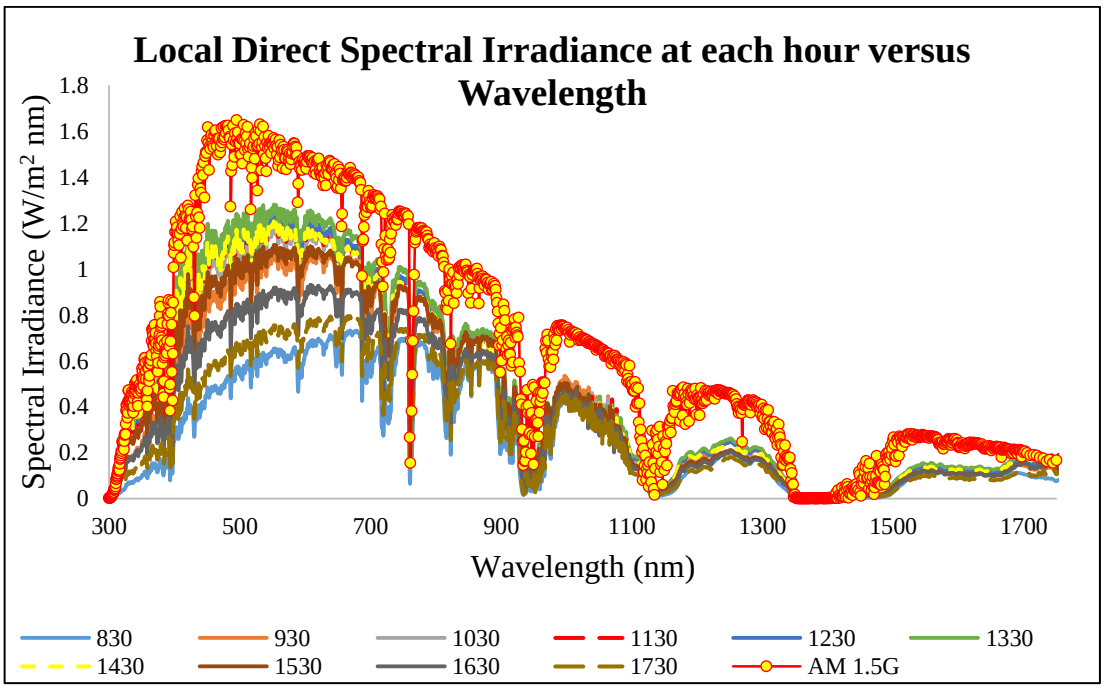

Figure 4.1: Local annual direct spectral irradiance at each hour (8.00 am - 6.00 pm) versus wavelength (the middle period for each hour, for example 830 denotes as 0800 – 0859 for convenience of results presentation)

Figure 4.1 shows the average of local annual direct spectral irradiance collected at each hour, under direct sunlight condition. The peak of the AM 1.5G was measured at the interval between 450 nm – 500 nm, while the peaks for the 10 hours local direct spectral irradiance were calculated to be red-shifted, with respect to AM 1.5G. The deviation was expected due to the conditions in Kajang, Malaysia (in terms of local spatial and atmospheric conditions) are different as compared to USA. By comparing the spectral irradiances data under the clear day condition, the morning and the evening spectrums were appeared to be red-shifted, with respect to the afternoon spectrum, as illustrated in Figure 4.1, and the corresponding weightage of each hour was calculated and shown in Table A.1 and Table A.2. The red-shifted of the respective spectrums was due to higher air mass (*AM*) in the morning and evening hours than the *AM* in the noon hours. Higher *AM* means longer actual path distance that the Sun's rays have to travel to the ground (Kasap, 2001). Majority of the shorter wavelength photons was scattered due to Rayleigh scattering (Guechi, 2013) at higher *AM*, and part of the incident photons would be absorbed by the water vapour in the air along the way, which prompting red-shifts and intensity decrease in the local direct spectral irradiance.

Figure 4.2 displays the average of local annual diffuse spectral irradiance for each hour, under diffuse sunlight condition. The intensity peaks of the diffuse spectral irradiance were significantly smaller compared to direct spectral irradiance, and also the AM 1.5G. Hence, it is difficult to display the comparison between local diffuse spectral irradiances and the AM 1.5G spectrum together under the same result's frame. The intensity's pattern of the local hourly-diffuse spectral irradiance were noticed to be not following the trend as in local direct spectral irradiance, due to the fast-varying cloud thickness upon the data being collected. From Figure 4.2, all the average local diffuse spectral irradiances were noticed to have peaked at the wavelength interval between 500 nm – 550 nm, which were red-shifted as compared to AM 1.5G spectrum, but blue-shifted compared to local direct spectral irradiance. The blue-shifting of spectral irradiances with respect to clear day condition indicates that the higher energy photons (near ultraviolet region) are more likely to penetrate through the clouds (S. Nann & C. Riordan, 1991), as compared to lower energy photons (near infrared region) that have a lower penetration probability under cloudy (overcast) condition.

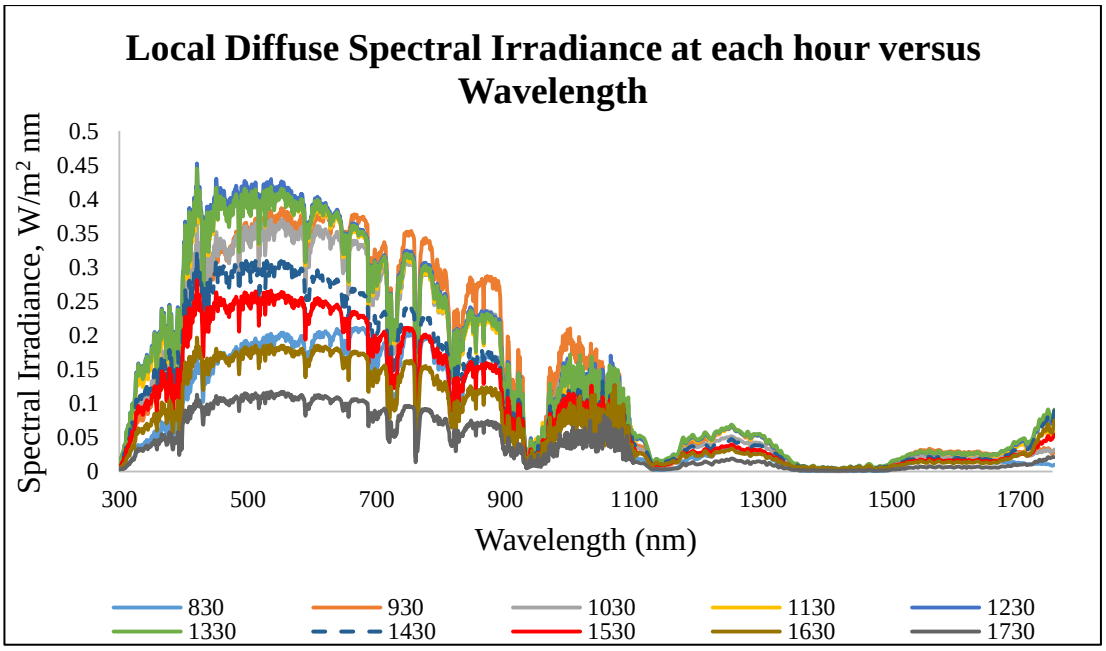

Figure 4.2: Local diffuse spectral irradiance at each hour (8.00 am - 6.00 pm) versus wavelength (the middle period for each hour, for example 830 denotes as 0800 – 0859 for convenience of results presentation)

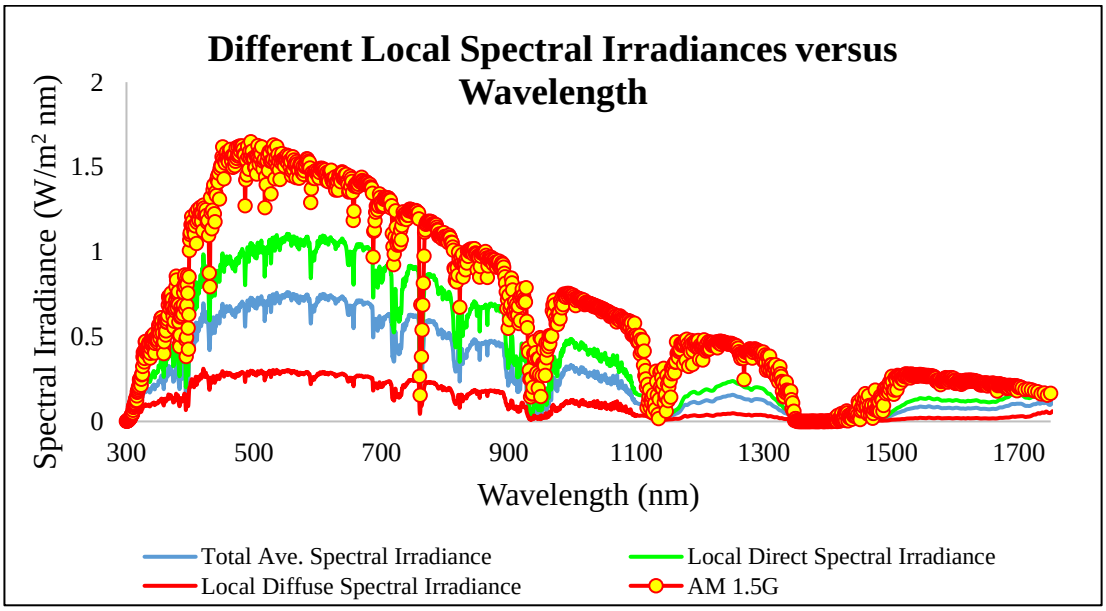

Figure 4.3: Local spectral irradiances collected in total average (blue line), local direct (green line), and local diffuse (red line), by comparing to AM 1.5G (yellow-red marker)

A comparison of annual spectral irradiance in total average, total direct, total diffuse, and also AM 1.5G were plotted as shown in Figure 4.3 (published in (Chong,

2016)). The integrated spectral irradiance (*ISI*) for total average, total direct, and also total diffuse are 408.36 W/m^2, 596.81 W/m^2, and 156.72 W/m^2 respectively, by taking wavelength range between 280 nm – 1750 nm. The *ISI* value calculated for AM 1.5G under the same wavelength range is 954.54 W/m^2. The monthly average solar radiation, P_{month} (by taking local total average *ISI*) in Malaysia is calculated at 441.03 MJ/m^2 (the reported monthly P_{month} in Malaysia is at 400 – 600 MJ/m^2 (S. Mekhilef et al., 2012)), and the calculation was shown as follow:

$$P_{month} = \frac{408.36\ \text{W}}{\text{m}^2} \times \frac{3600\ \text{s}}{\text{hr}} \times \frac{10\ \text{hrs}}{\text{day}} \times \frac{30\ \text{days}}{\text{month}} = \frac{441.03\ \text{MJ}}{\text{m}^2\ \ \text{month}}$$

Table 4.1: Weightage of each specific wavelength range of various spectral irradiances (300 nm – 1100 nm)

Wavelength range (nm)	**Weightage for Specific Wavelength Range**			
	Total Ave.	**Total Direct**	**Total Diffuse**	**AM 1.5G**
300 – 350	0.1646	0.1558	0.2066	0.1704
350 – 400	0.4636	0.4445	0.5531	0.5289
400 – 450	0.7792	0.7603	0.8646	0.8612
450 – 500	0.9362	0.9233	0.9909	**1.0000**
500 – 550	0.9802	0.9743	**1.0000**	0.9937
550 – 600	**1.0000**	**1.0000**	0.9908	0.9712
600 – 650	0.9486	0.9533	0.9169	0.9131
650 – 700	0.8325	0.8407	0.7845	0.8509
700 – 750	0.8095	0.8153	0.7733	0.8105
750 – 800	0.7651	0.7688	0.7399	0.7430
800 – 850	0.6248	0.6296	0.5955	0.6333
850 – 900	0.4708	0.4771	0.4359	0.5271
900 – 950	0.2115	0.2170	0.1824	0.2866
950 – 1000	0.2483	0.2530	0.2227	0.2843
1000 – 1050	0.3928	0.3999	0.3542	0.4477
1050 – 1100	0.2524	0.2584	0.2205	0.3673

Table 4.1 shows the weightage of local spectral irradiances and AM 1.5G between 300 nm – 1100 nm. For the total average and total direct spectral irradiances, the peaks were calculated at the interval between 550 nm – 600 nm; total diffuse was calculated at 500 nm – 550 nm; while AM 1.5G spectrum were calculated at 450 nm – 500 nm. The spectral irradiances under this wavelength range were chosen for analysis as it covered up most of the *OSCs*' spectral response region. The pattern of the local spectral irradiances was noticed to have sharp drops in intensity near to 724 nm, 824 nm, 938 nm, and 1120 nm wavelength (as shown in Figure 4.3), which due to the absorption of these wavelength photons by water vapour content in the air or in the clouds (S. Nann & C. Riordan, 1991) under clear day and cloudy conditions. The drop in intensity was obviously shown in the weightage numbers at 900 – 950 nm. For the sharp drops in other wavelength intervals (as shown in Table 4.1), due to large step size of the wavelength (50 nm) involved in the weightage calculations, the respective weightage is not obvious as it only occurred at narrow wavelength width.

4.2 Organic materials' performance under illumination of standard reference spectrum AM 1.5G

Spectral irradiance is one of the critical factors in determining the device performance (in terms of *PCE*) due to the various spectral response region for different combination of polymer electron donor and polymer electron acceptor have in the active layer. The analysis of organic materials begun with by subjecting each of them into the illumination of AM 1.5G spectrum at 100 mW/cm^2, which were conducted by the experimental groups [(Fan, 2014); (Morinaka, 2013); (R. Lin, 2014); (Liu, 2014)]. This step is crucial for obtaining the device quantum efficiency (*QE*) under standard condition, as the *QE* values would be used in the following sections where the organic materials would be subjected into illumination of different local spectral irradiances. The external quantum efficiency (*EQE*) for each organic material under the illumination of AM 1.5G is shown in Figure 4.4. For the theoretical study purpose, the *EQE* values were obtained based on curve fitting on the *EQE*'s graphs of the organic materials published by the experimental groups.

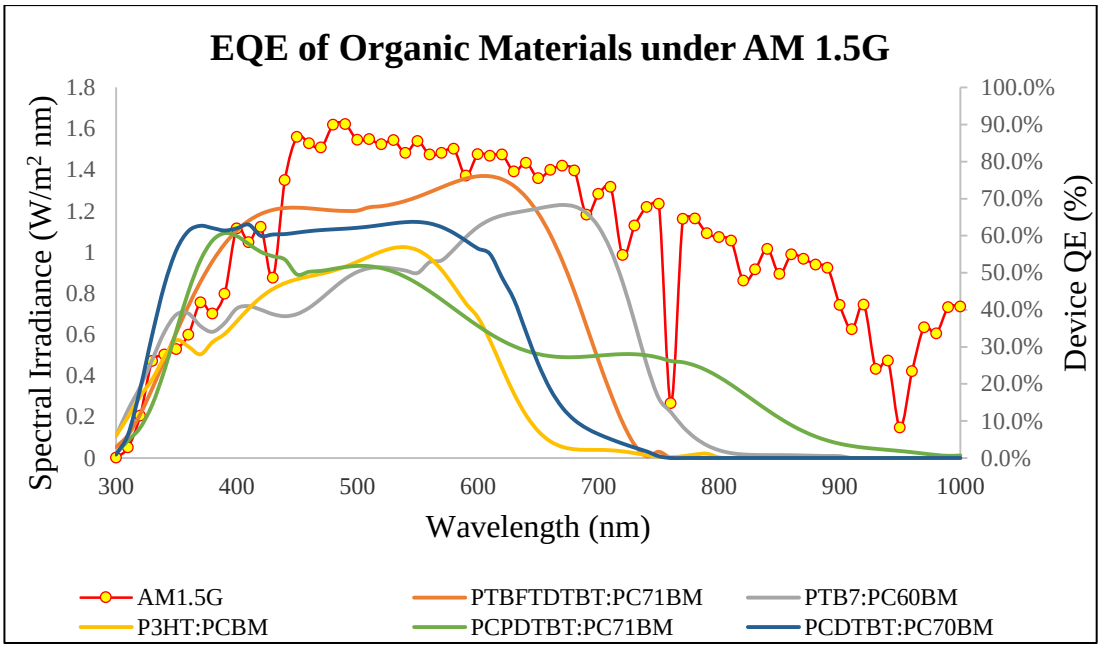

Figure 4.4: External Quantum Efficiency (*EQE*) of organic materials under the illumination of AM 1.5G spectrum (The yellow-red marker is AM 1.5G spectrum, while the coloured smooth lines are device *QE*)

As shown in Figure 4.4, the capability for each of the organic materials' group to convert incoming photons (under various wavelengths) to free electron-hole pairs (*EHPs*), which partly due to the differences in bandgap of the involved organic materials. The corresponding device responsivity for the wavelength range (300 nm – 1000 nm) were calculated and shown in Figure 4.5. From Figure 4.4, although some organic materials having high device *QE* at the near-ultraviolet (*UV*) region (300 nm – 400 nm), such as [PTBFTDTBT:$PC_{71}BM$], [PCPDTBT:$PC_{71}BM$], and [PCDTBT:$PC_{70}BM$], due to low spectral intensity at this near-*UV* region, the collectable *EHPs* generated in this region is comparatively less, with respect to visible (*VIS*) region. By multiplying the AM 1.5G spectrum with device responsivity of each of the organic materials, the current densities (in the function of wavelength) would be obtained, as shown in Figure 4.6.

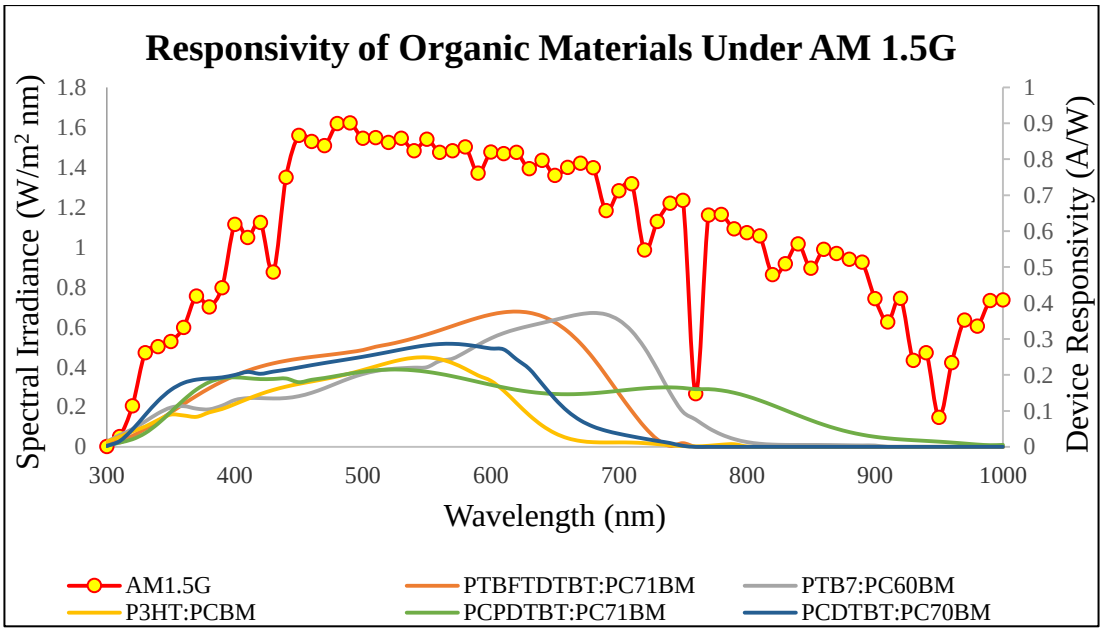

Figure 4.5: Responsivity of organic materials under the illumination of AM 1.5G spectrum (The yellow-red marker is AM 1.5G spectrum, while the coloured smooth lines are device responsivity)

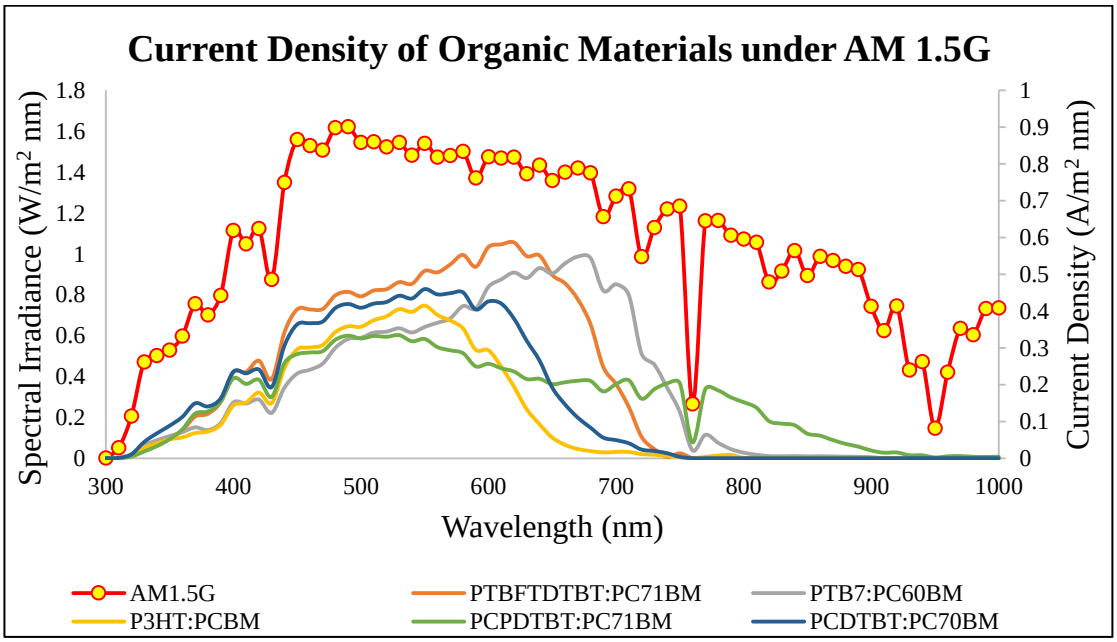

Figure 4.6: Current density (in the function of wavelength) of each of the organic materials under illumination of AM 1.5G (The yellow-red marker is AM 1.5G spectrum, while the coloured smooth lines are device current density)

The short circuit currents for each of the organic materials were then calculated, by summing up the current density with the wavelength step size of 10 nm. The values of the open-circuit voltage (V_{OC}) and also the fill factor (*FF*) of each of the organic materials were based on the results published [(Fan, 2014); (Morinaka, 2013); (R. Lin, 2014); (Liu, 2014)]. The set of parameters that required for the calculation of *PCE* were then obtained and are shown in Table 4.2. Reference *PCE* (%) were obtained from the published results, the *PCEs*' values here are calculated based on curve fitting on the *EQE*'s graphs, and the deviation shows the difference in the newly calculated *PCEs* and the published *PCEs*' values.

Table 4.2: Various organic solar materials' photovoltaic data under the illumination of AM 1.5G (Improvement of PCE was done with respect to published AM 1.5G)

Organic Materials	**V_{OC} (V)**	**J_{SC} (mA/cm^2)**	**FF (%)**	**PCE (%)**	**Reference PCE (%)**	**Deviation (%)**
PTBFTDTBT :$PC_{71}BM$	0.80	14.21	51.4	5.79	5.84	0.90
PTB7: $PC_{60}BM$	0.76	13.28	62.0	6.27	6.24	0.41
P3HT: $PC_{60}BM$	0.61	7.84	69.0	3.19	3.27	2.35
PCPDTBT: $PC_{71}BM$	0.63	11.10	42.2	3.05	2.93	4.17
PCDTBT: $PC_{70}BM$	0.88	10.80	49.0	4.62	4.66	0.89

The small deviations (<5% error) between the calculated *PCEs*' values with respect to published *PCEs*' values under illumination of AM 1.5G spectrum for each organic material are shown in Table 4.2. This suggests that the method of using curve fitting on the published *EQE*'s graphs to generate similar results (on device *QE*) could be one of the methods to study the performance of various organic materials theoretically, without having to purchase all the materials beforehand as it will involve

a large budget amount and also long periods of experimental duration to produce similar results. Among the 5 organic materials' groups, the combination between PTB7:$PC_{60}BM$ showing the best performance under the illumination of AM 1.5G spectrum. The reasons for its best performance in *PCE* can be deduced that it's having larger spectral response region as compare to other organic materials, under the illumination of AM 1.5G spectrum.

4.3 Organic materials' performance under illumination of various local spectral irradiances

The peaks of the spectral irradiances intensity under local weather conditions, as shown in Section 4.1, proved to have deviations with respect to the peak intensity of AM 1.5G spectrum. In order to clarify the effects of the deviation to the performance of 5 organic materials' groups, they would be subjected to 3 different local spectral irradiances' (local direct, local diffuse, and local total average) illuminations. The study of the spectral response region of the device were conducted by comparing the device *QE* (that obtained from curve fitting) and also device responsivity to respective local spectrums. The calculations of the device *QE* and also the device responsivity will be based on Equations (3) and (5). The $J_{SC}(\lambda)$ (current density in the function of wavelength) of each of the organic materials would then be obtained, by multiplying the device responsivity to various spectral irradiances. The $J_{SC}(\lambda)$ was then multiplying with wavelength step size of 10 nm, and totalled up to obtain J_{SC}. This method of calculations would applied to all 3 different spectral irradiances' illuminations. The corresponding photovoltaic data would be displayed to show the performance improvement of each of the organic materials under different local spectrums with respect to AM 1.5G. For the evaluation of the effect of various spectral irradiances of the performance of organic materials, the J_{SC} for each organic material were normalised to the published J_{SC} values. The conducting of this normalisation enables the direct extraction of V_{OC} and *FF* values in the published results, as it was proven that V_{OC} and *FF* are dependent on J_{SC} (Chong, 2016).

4.3.1 Local direct spectral irradiance illumination

The peak of local direct spectral irradiance was measured at 550 – 600 nm, and the *ISI* value was calculated to be 596.81 W/m^2. This shows there is a significant deviation, in terms of peak intensity with respect to AM 1.5G spectrum (peak intensity at 450 – 500 nm). By taking the device *QE* values obtained under illumination of AM 1.5G spectrum, the graphs of *EQE* and the device responsivity versus local direct spectral irradiance were plotted as shown in Figure 4.7 and Figure 4.8 respectively. By multiplying the local direct spectral irradiance with device responsivity of each of the organic materials, the corresponding current densities (in the function of wavelength) would be obtained, as shown in Figure 4.9. The photovoltaics' data of each of the organic materials based on the illumination under the local direct spectral irradiance are shown in Table 4.3. The improvement (%) in the Table 4.3 denotes for the percentage of improvement in terms of *PCE* values based on the illumination of local direct spectral irradiance, with respect to AM 1.5G illumination.

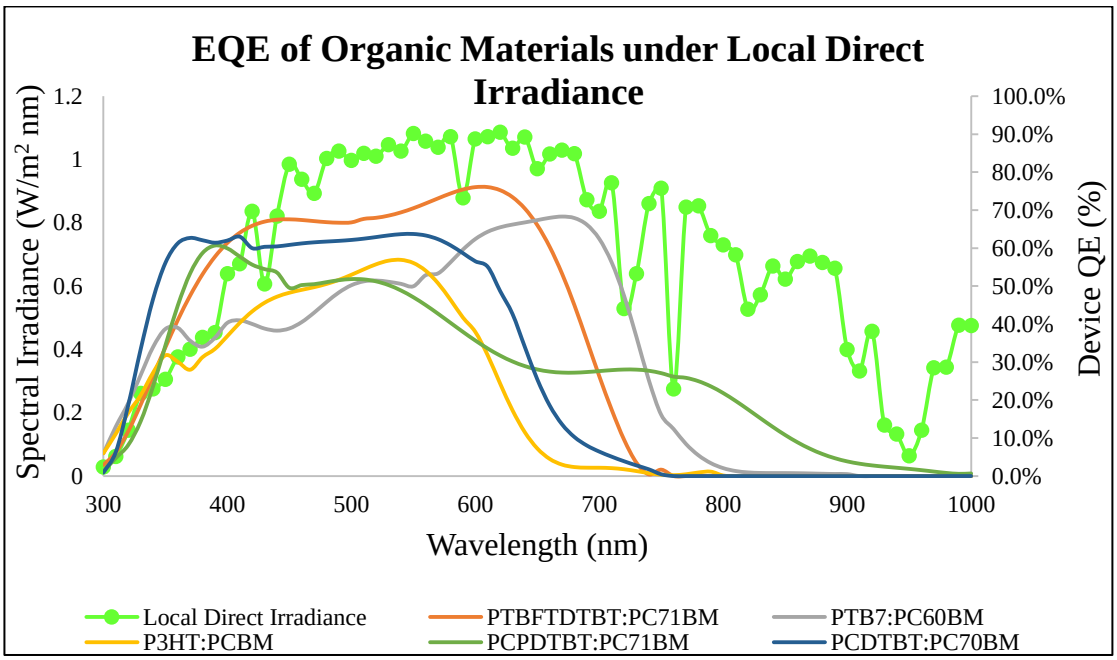

Figure 4.7: External Quantum Efficiency (EQE) of organic materials under the illumination of local direct spectral irradiance (green line with solid symbol denotes the local direct spectral irradiance, while the coloured smooth lines are device QE)

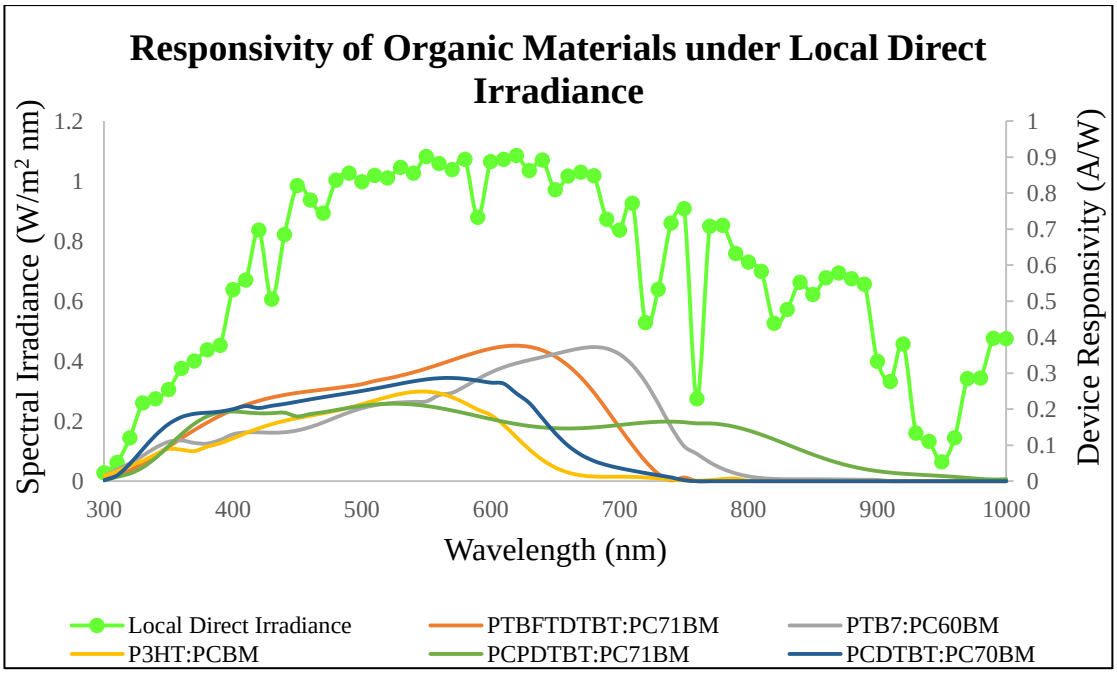

Figure 4.8: Responsivity of organic materials under the illumination of local direct spectral irradiance (green line with solid symbol denotes the local direct spectral irradiance, while the coloured smooth lines are device responsivity)

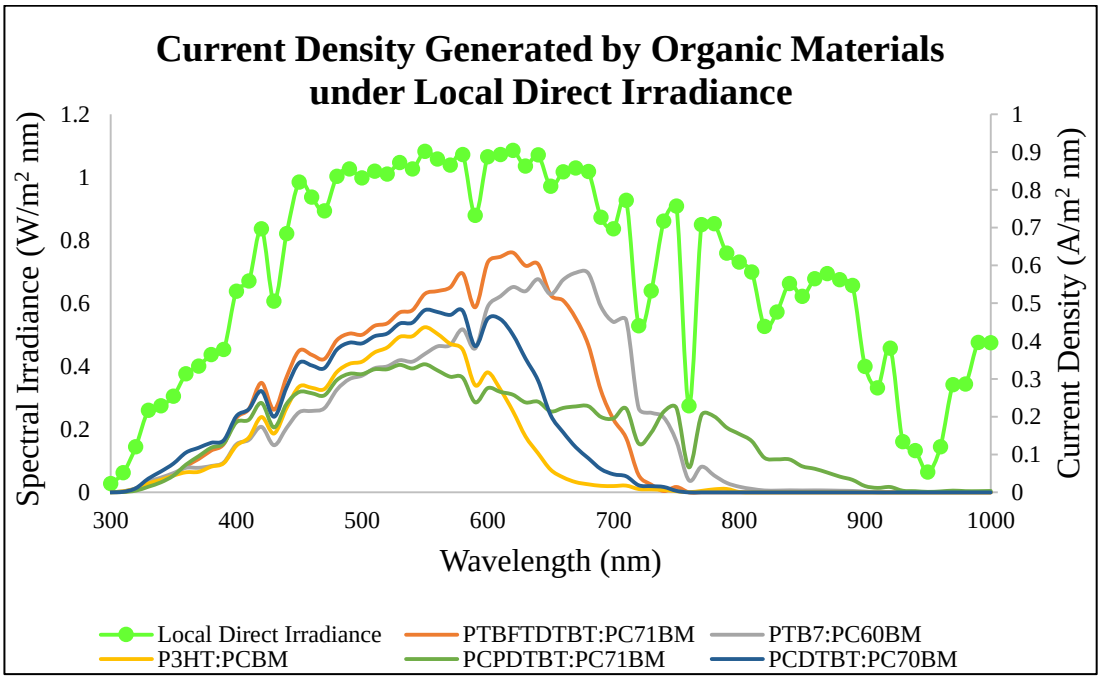

Figure 4.9: Current density (in the function of Wavelength) of each of the organic materials under illumination of local direct spectral irradiance (green line with solid symbol denotes the local direct spectral irradiance, while the coloured smooth lines are device current density)

Table 4.3: Various organic materials' photovoltaic data under the illumination of local direct spectral irradiance (Improvement of PCE compared to AM 1.5G)

Organic Materials	**V_{OC} (V)**	**J_{SC} (mA/cm^2)**	**FF (%)**	**PCE (%)**	**AM 1.5G PCE (%)**	**Improvement (%)**
PTBFTDTBT :$PC_{71}BM$	0.80	14.21	51.4	6.31	5.79	8.97
PTB7: $PC_{60}BM$	0.76	13.28	62.0	6.86	6.27	9.48
P3HT: $PC_{60}BM$	0.61	7.84	69.0	3.41	3.19	6.69
PCPDTBT: $PC_{71}BM$	0.63	11.10	42.2	3.28	3.05	7.45
PCDTBT: $PC_{70}BM$	0.88	10.80	49.0	4.95	4.62	7.16

Based on the photovoltaic results obtained and shown in Table 4.3, on average, each of the organic materials' group has experienced improvement under the local direct spectral irradiance illumination, with respect to AM 1.5G. Among the 5 organic materials' groups, [PTB7:$PC_{60}BM$] and [PTBFTDTBT:$PC_{71}BM$] groups were calculated to have 9.48% and 8.97% in improvement respectively, which were the first and second highest improvement on the list. The reason for their improvement may due to the red-shifted of the local direct irradiance with respect to AM 1.5G spectrum, where the peak of the local direct spectrum is closer to the peak of the organic materials' spectral response region. However, owing to larger spectral response width (as shown in Figure 4.8) of [PTB7:$PC_{60}BM$] has (300 nm – 900 nm), as compared to [PTBFTDTBT:$PC_{71}BM$] (300 nm – 750 nm), thus more photons would be absorbed and converted to *EHPs* by the former organic materials than the latter. This led to higher calculated *PCE* values for [PTB7:$PC_{60}BM$] than [PTBFTDTBT:$PC_{71}BM$], which were 6.86% and 6.31% respectively.

4.3.2 Local diffuse spectral irradiance illumination

The peak intensity of local diffuse spectral irradiance was measured at 500 – 550 nm, which was red-shifted with respect to AM 1.5G by about 50 nm, but it was blue-shifted with respect to local direct and local total average spectral irradiances by 50 nm (as shown in Table 4.1). The *ISI* value calculated under local diffuse spectral irradiance illumination is 156.72 W/m^2. The device *QE* and the device responsivity are plotted versus the local diffuse spectral irradiance, as shown in Figure 4.10 and Figure 4.11. The current densities that generated from the organic materials under the illumination of local diffuse irradiance is plotted in Figure 4.12. The corresponding photovoltaics' data are then obtained for the 5 organic materials' groups and shown in Table 4.4. The percentage of improvement for each of the organic materials' group is done by comparing the respective *PCE* values with the *PCE* values obtained in AM 1.5G; while the improvement percentage in Table 4.5 is comparing to local direct spectral irradiance.

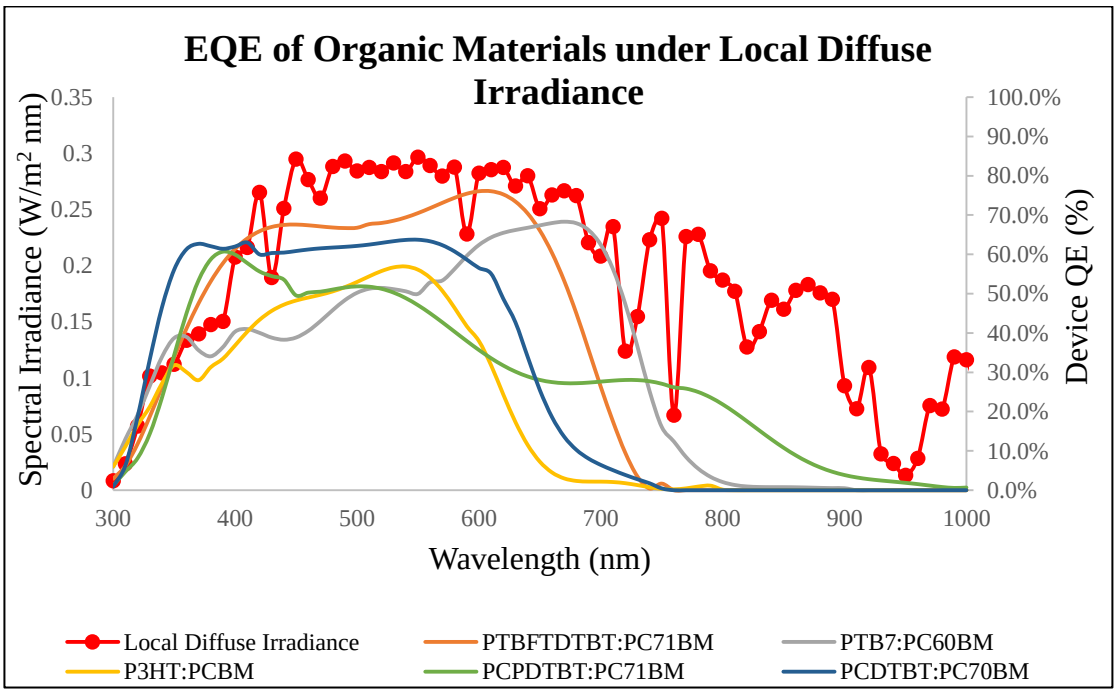

Figure 4.10: External Quantum Efficiency (EQE) of organic materials under the illumination of local diffuse spectral irradiance (red line with solid symbol denotes the local diffuse spectral irradiance, while the coloured smooth lines are device QE)

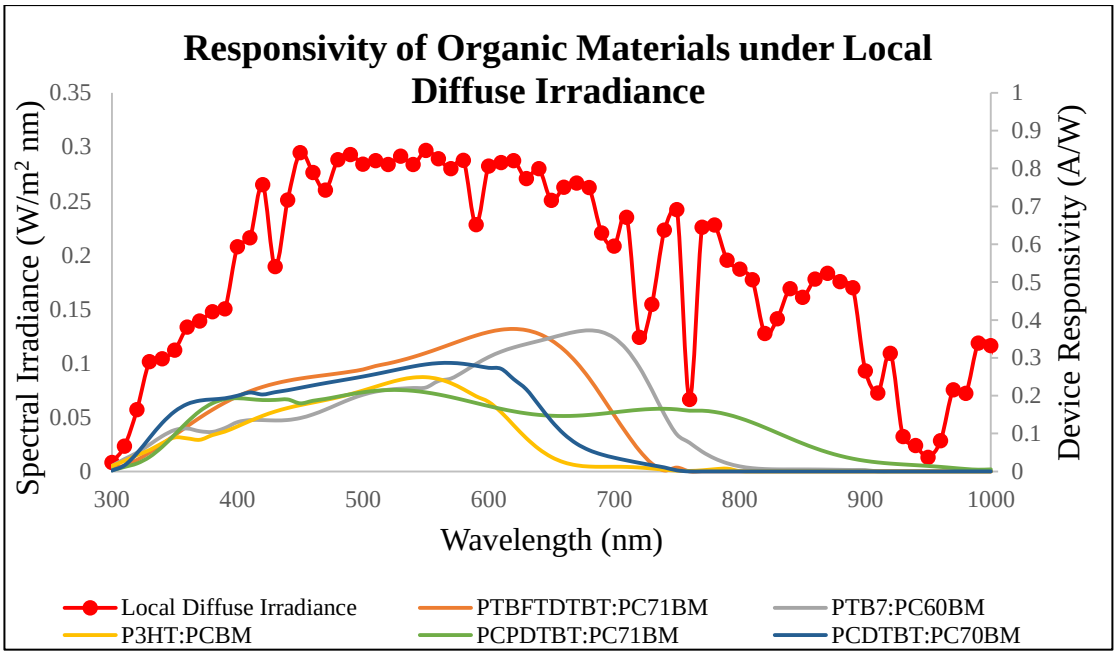

Figure 4.11: Responsivity of organic materials under the illumination of local diffuse spectral irradiance (red line with solid symbol denotes the local diffuse spectral irradiance, while the coloured smooth lines are device responsivity)

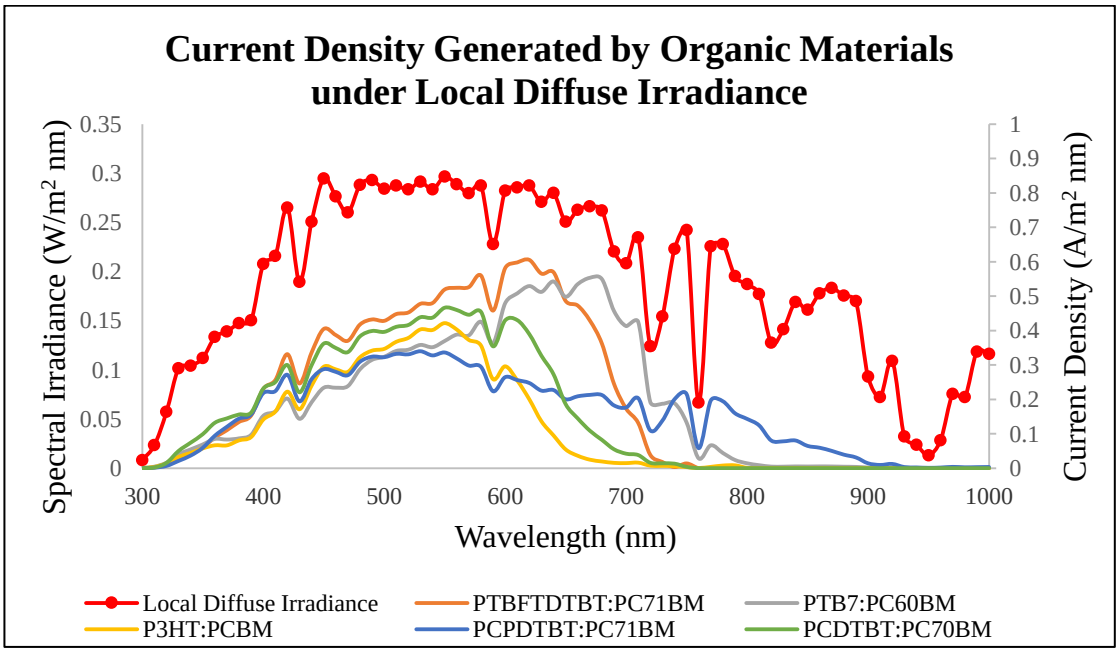

Figure 4.12: Current density (in the function of wavelength) of each of the organic materials under illumination of local diffuse spectral irradiance (red line with solid symbol denotes the local diffuse spectral irradiance, while the coloured smooth lines are device current density)

Table 4.4: Various organic materials' photovoltaic data under the illumination of local diffuse spectral irradiance (Improvement of PCE compared to AM 1.5G)

Organic Materials	**V_{OC} (V)**	**J_{SC} (mA/cm^2)**	**FF (%)**	**PCE (%)**	**AM 1.5G PCE (%)**	**Improvement (%)**
PTBFTDTBT :$PC_{71}BM$	0.80	14.21	51.4	6.66	5.79	15.03
PTB7: $PC_{60}BM$	0.76	13.28	62.0	7.09	6.27	13.23
P3HT: $PC_{60}BM$	0.61	7.84	69.0	3.68	3.19	15.39
PCPDTBT: $PC_{71}BM$	0.63	11.10	42.2	3.45	3.05	13.03
PCDTBT: $PC_{70}BM$	0.88	10.80	49.0	5.34	4.62	15.61

Table 4.5: Various organic materials' photovoltaic data under the illumination of local diffuse spectral irradiance (Improvement of PCE compared to local direct spectral irradiance PCE (L. Direct PCE))

Organic Materials	**V_{OC} (V)**	**J_{SC} (mA/cm^2)**	**FF (%)**	**PCE (%)**	**L. Direct PCE (%)**	**Improvement (%)**
PTBFTDTBT :$PC_{71}BM$	0.80	14.21	51.4	6.66	6.31	5.56
PTB7: $PC_{60}BM$	0.76	13.28	62.0	7.09	6.86	3.42
P3HT: $PC_{60}BM$	0.61	7.84	69.0	3.68	3.41	8.15
PCPDTBT: $PC_{71}BM$	0.63	11.10	42.2	3.45	3.28	5.19
PCDTBT: $PC_{70}BM$	0.88	10.80	49.0	5.34	4.95	7.89

As shown from Table 4.4, the calculated results for the performance of organic materials under the illumination of local diffuse spectral irradiance having a great improvement with respect to AM 1.5G, whereby all of them having an improvement in performance with more than 13%. The high improvement in *PCE* values may be due to peak intensities shifting in the local diffuse spectral irradiance, where the intensities of the spectral irradiances at the peak of the red-shifted region were more favourable to the spectral response region of the studied organic materials' groups.

Positive performance improvement was calculated for the relevant organic materials' groups with respect to the local direct irradiance illumination (as shown in Table 4.5). The explanations for it, other than it appeared that local diffuse spectral irradiance is more favourable to the spectral response region of respective organic materials, the higher average photon energy (*APE*) values of the incoming photons under overcast condition (1.75 eV) as compared to clear day condition (1.65 eV) were recorded at the site. During overcast condition, different thickness of clouds may have blocked the transmission of the majority lower energy photons (longer wavelength photons) to the ground's surface; while the higher energy photons (shorter wavelength photons) having a relatively higher transmission probability than the lower energy photons by about 30% (S. Nann & C. Riordan, 1991). The spectral gain in performance of solar cells [amorphous-silicon module] with a narrow spectral response width (330 nm – 810 nm) on the outdoor performance was also shown to have 15% gain with respect to AM 1.5G under local overcast condition (Nofuentes, 2014). This indicates that the illumination of local cloudy condition under same intensity (after normalisation) will be more beneficial to the *OSCs* that consist of narrow spectral response width, as compared with AM 1.5G spectrum and local direct spectral irradiance.

4.3.3 Local total average spectral irradiance illumination

The peak intensity of local total average spectral irradiance was measured at 550 nm – 600 nm (similar to local direct spectral irradiance), which was red-shifted with respect to AM 1.5G by about 100 nm. The calculated *ISI* value for it is 408.36 W/m^2.

The local total average spectral irradiance is averaging all the spectrum data (including direct and diffuse conditions) obtained at 8.00 am – 6.00 pm. The device *QE* and also the device responsivity under illumination of local total average spectral irradiance were plotted in Figure 4.13 and Figure 4.14, respectively. The corresponding current density values and also photovoltaic data for each of the organic materials are illustrated in Figure 4.15 and Table 4.6 respectively.

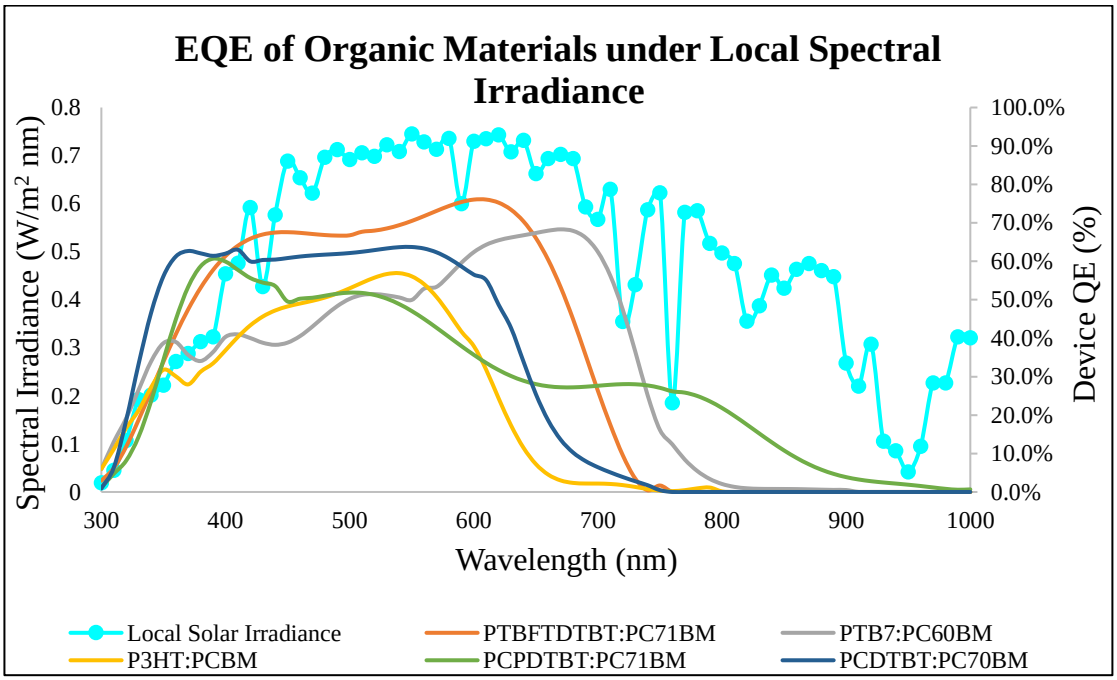

Figure 4.13: External Quantum Efficiency (EQE) of organic materials under the illumination of local total average spectral irradiance (light-blue line with solid symbol denotes the local total average spectral irradiance, while the coloured smooth lines are device QE)

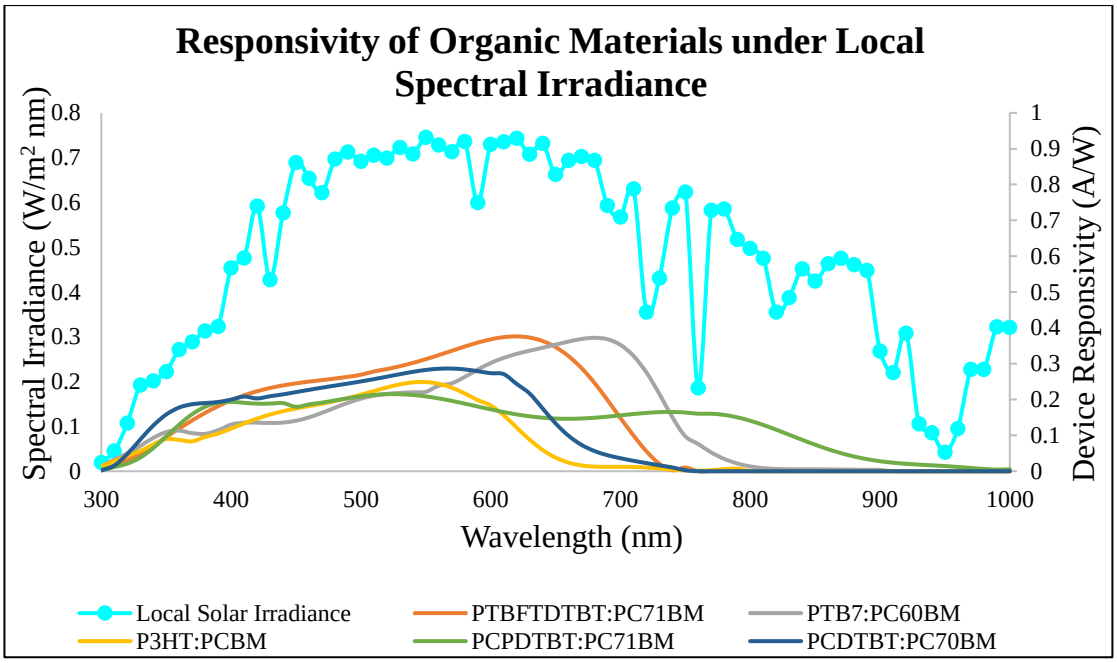

Figure 4.14: Responsivity of organic materials under the illumination of local total average spectral irradiance (light-blue line with solid symbol denotes the local total average spectral irradiance, while the coloured smooth lines are device responsivity)

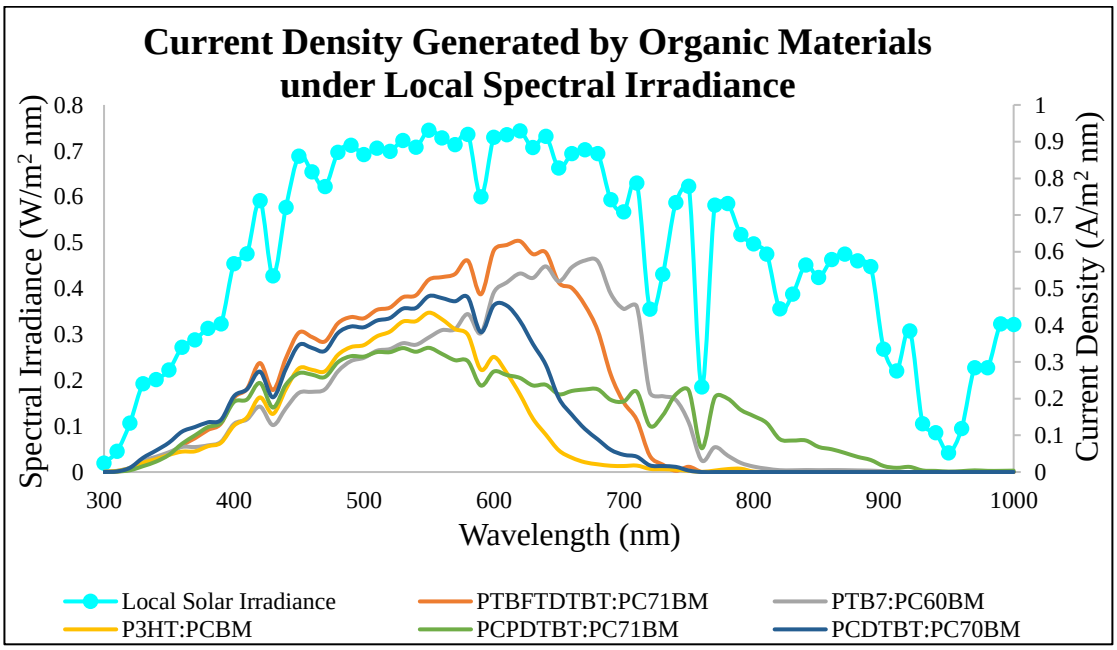

Figure 4.15: Current density (in the function of Wavelength) of each of the organic materials under illumination of local total average spectral irradiance (light-blue line with solid symbol denotes the local total average spectral irradiance, while the coloured smooth lines are device current density)

Table 4.6: Various organic solar cells' photovoltaic data under the illumination of local total average spectral irradiance (Improvement of PCE compared to AM 1.5G)

Organic Materials	**V_{OC} (V)**	**J_{SC} (mA/cm^2)**	**FF (%)**	**PCE (%)**	**AM 1.5G PCE (%)**	**Improvement (%)**
PTBFTDTBT :$PC_{71}BM$	0.80	14.21	51.4	6.36	5.79	9.97
PTB7: $PC_{60}BM$	0.76	13.28	62.0	6.90	6.27	10.10
P3HT: $PC_{60}BM$	0.61	7.84	69.0	3.45	3.19	8.12
PCPDTBT: $PC_{71}BM$	0.63	11.10	42.2	3.31	3.05	8.37
PCDTBT: $PC_{70}BM$	0.88	10.80	49.0	5.01	4.62	8.55

The *PCE* values and the percentage of improvement with respect to AM 1.5G obtained in each of the organic materials under the illumination of local total average spectral irradiance shown in Table 4.6 are similar to the results obtained under the illumination of local direct spectral irradiance, with the former illumination producing slightly better results than the latter illumination due to the inclusion of local diffuse spectral irradiance. The nearly similar results obtained under these 2 types of illuminations are due to the patterns of the 2 spectral irradiances are identical, in terms of the wavelength interval where the peak intensities of the spectral irradiance located (as shown in Figure 4.3).

4.3.4 Summary of the organic materials' performance under different spectral irradiance illumination conditions

The summary of the *PCE* values obtained for each organic material that subjected to different spectral irradiances' illuminations and the percentage of improvement are

shown in Table 4.7 and Table 4.8 respectively. From the tables, L. Direct S. I. denotes local direct spectral irradiance; L. Diffuse S. I. denotes local diffuse spectral irradiance; L. Total Ave. S. I. denotes local total average spectral irradiance.

Table 4.7: Power conversion efficiency (%) of each of the organic materials subjected to different spectral irradiance illuminations

		Organic Materials Power Conversion Efficiency (%)				
		PTBFTDTBT: $PC_{71}BM$	**PTB7: $PC_{60}BM$**	**P3HT: $PC_{60}BM$**	**PCPDTBT: $PC_{71}BM$**	**PCDTBT :$PC_{70}BM$**
Conditions	**AM 1.5G**	5.79	6.27	3.19	3.05	4.62
	L. Direct S. I.	6.31	6.86	3.41	3.28	4.95
	L. Diffuse S. I.	6.66	7.09	3.68	3.45	5.34
	L. Total Ave. S. I.	6.36	6.90	3.45	3.31	5.01

Table 4.8: Power conversion efficiency (%) improvement of each of the organic materials with respect to AM 1.5G Spectrum

		Organic Materials PCE Improvement (%)				
		PTBFTDTBT: $PC_{71}BM$	**PTB7: $PC_{60}BM$**	**P3HT: $PC_{60}BM$**	**PCPDTBT: $PC_{71}BM$**	**PCDTBT :$PC_{70}BM$**
Conditions	**L. Direct S. I.**	8.97	9.48	6.69	7.45	7.16
	L. Diffuse S. I.	15.03	13.23	15.39	13.03	15.61
	L. Total Ave. S. I.	9.97	10.10	8.12	8.37	8.55

As shown in Table 4.7, based on the power conversion efficiency of each of the studied organic materials, the best candidate for the designation of the organic solar

cells' active layer in ASEAN region would be [PTB7: $PC_{60}BM$], with the recorded *PCE* value of 6.90% under the illumination of local total average spectral irradiance. The high *PCE* values that [PTB7: $PC_{60}BM$] able to generate when subjected to the total average of local spectral irradiances was mainly due to its large spectral response region, and the red-shifted local spectral irradiance with respect to AM 1.5G spectrum was favoured to the organic materials itself. The improvement of [PTB7: $PC_{60}BM$] also shown to be the greatest among the 5 organic groups under local total average spectral irradiance's illumination (shown in Table 4.8), which calculated to be 10.10%.

4.4 Local average photon energy distribution

The effect of the various local spectral irradiance illuminations to the performance of organic solar cells (organic materials) have been shown in the results in the previous section. Apart from the local spectral irradiances, there is another parameter which is worth to be considered, the average photon energy (*APE*) index. As aforementioned in Section 2.3, the solar cells that having a narrow spectral response width would be affected by the local *APE* index. Since majority of the *OSCs* having narrow spectral response width, it is thus necessary to understand the distribution of the local *APE* values, as it may be one of the significant factors that affects the performance of *OSCs*. Figure 4.16 displays the distribution of *APE* index based on separated local direct and local diffuse spectral irradiances. The *APE* index for the standard spectrum AM 1.5G for the spectral range between 280 nm – 1750 nm was calculated to be 1.59 eV. The highest occurrence of *APE* index for the local direct spectral irradiance was calculated at 1.63 eV; while the local diffuse spectral irradiance was calculated at 1.71 eV.

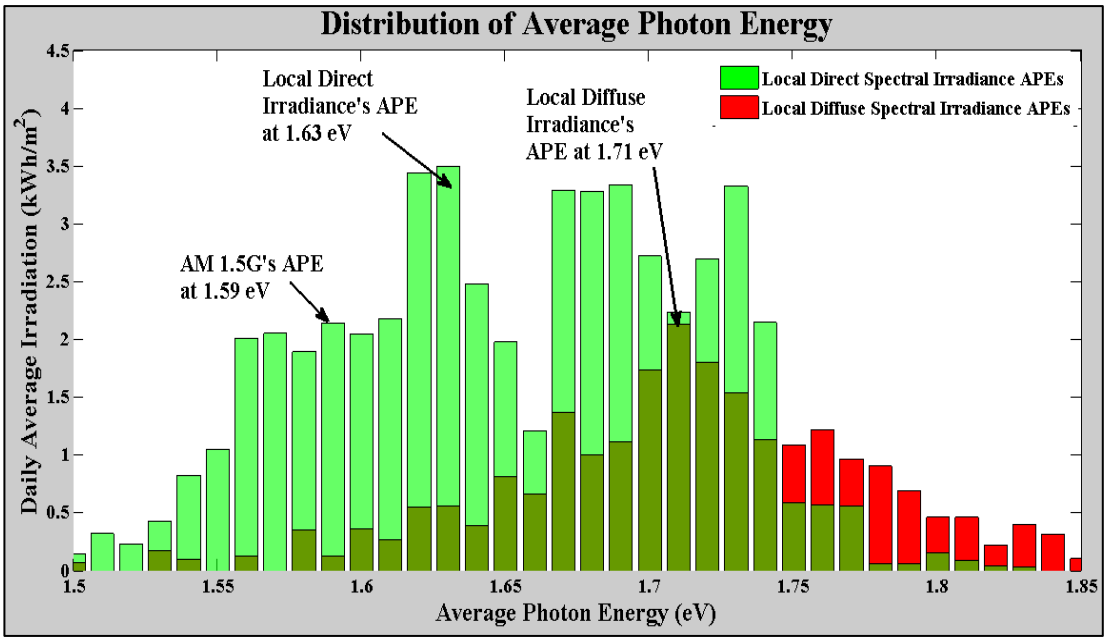

Figure 4.16: Distribution of average photon energy (APE) for local direct and local diffuse spectral irradiances (green bars indicate local direct irradiance APEs; red bars indicate local diffuse irradiance APEs)

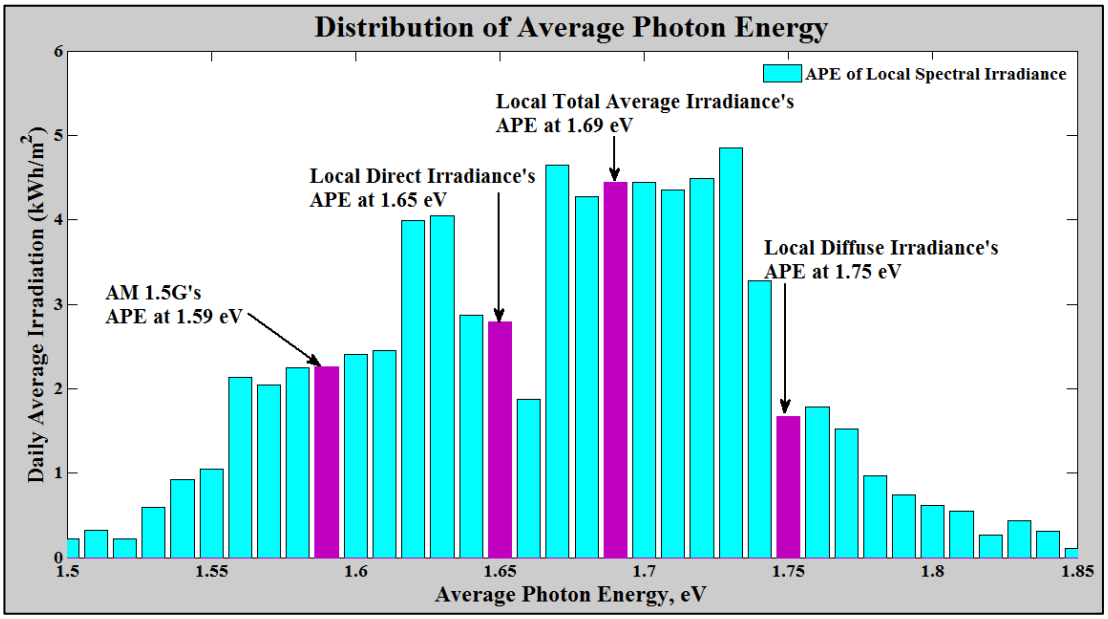

Figure 4.17: Distribution of average photon energy (APE) under local total average spectral irradiance illumination

As illustrated from Figure 4.17, the calculated average *APE* values for local direct spectral irradiance, local diffuse spectral irradiance, and local total average spectral irradiance are 1.65 eV, 1.75 eV, and 1.69 eV respectively. The variations in the *APE* values that calculated based on different local weather conditions, is due to the fact that the spectral irradiance is heavily dependent on the cloud coverage in the air (C. Cornaro & A. Andreotti, 2013). As aforementioned in Section 4.3.2, the considerations that made by Naan and Riordan about the blue enrichment in the spectral irradiance interval will occur under overcast condition. This is due to the fact that higher energy photons consist relative higher transmission probability than the lower energy photons by 30%, which lead to higher *APE* values obtained under local cloudy condition than in local clear day condition. In addition to local cloudy conditions, the high air humidity level (70% - 90%) in Malaysia that causes radiation of sunlight near specific wavelengths would be absorbed by the water vapour during clear day conditions (as mentioned in Section 4.1). This leads to 83.72% of the *APE* values obtained locally at Kajang, Malaysia are higher than the AM 1.5G *APE* at 1.59 eV. This indicates that *APE* values are more dependent on the patterns of local spectral irradiances that shaped by water vapour absorption near specific wavelengths and also the weather conditions, as compared to the calculated *ISI* values.

4.5 Probability of getting direct spectral irradiance during daytime

The average annual temperature (29˚C) that recorded in Malaysia (Underground, 2016) is higher than the standard ambient temperature of 20˚C, which taken by American Society for Testing and Materials for AM 1.5G calculation. This often led to the formation of clouds or raining in the noon hours till evening hours, due to evaporation of water happened in the earlier part of the day. The probability of having direct sunlight throughout the day during the project data collection (January 2016 – July 2016) that conducted on the site is displayed in Figure 4.18. As shown from the results in Figure 4.18, the probability of getting direct spectral irradiance data is high in the morning (more than 70% at 9.00 am – 11.00 am), but the probability shown some reduction in the noon (around 50% to 60% at 12.00 pm – 2.00 pm), and finally a great scaling down in probability having direct sunlight was observed in the late evening

(less than 35% at 4.00 pm – 6.00 pm). The percentage of having local direct sunlight data is 57.18%; while local overcast condition data comprised of 42.82% of the total spectrum data collected. This indicates ASEAN countries that have high average annual temperature, such as Malaysia, Singapore, Brunei, and Indonesia, will appear to have cloudy or rainy conditions in the noon to until the evening, which will significantly affect the local spectral irradiances. Furthermore, those cities that near to the seaside in ASEAN region will experience even more overcast weather during the monsoon or interchanged of monsoon seasons (Varikoden, 2011).

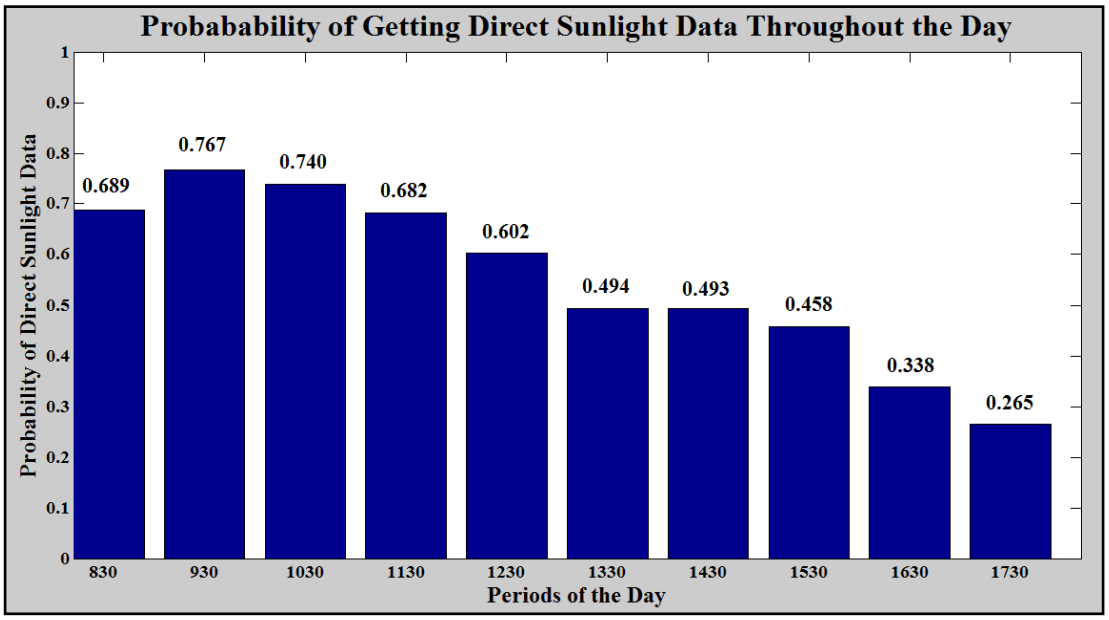

Figure 4.18: Probability of having direct sunlight throughout the day on the site at Universiti Tunku Abdul Rahman (UTAR), Kajang, Malaysia (the middle period for each hour, for example 830 denotes as 0800 – 0859 for convenience of results presentation)

CHAPTER 5

CONCLUSIONS AND RECOMMENDATIONS

In conclusion, the best organic material selection for this project was conducted through the on-site measurement to obtain the information about annual local spectral irradiances, and theoretical study of the performance of organic solar cells (or organic materials) subjected to illumination of various spectral irradiance under same intensity through normalization process. The annual local spectral irradiances, which comprised of local direct, local diffuse, and local total average spectral irradiances, showing significant deviations with respect to standard AM 1.5G spectrum in terms of peak intensity. The peak intensities of the local direct, local diffuse, and local total average spectral irradiances were calculated at 550 – 600 nm, 500 – 550 nm, and 550 – 600 nm, respectively; while the peak intensity of the AM 1.5G spectrum was calculated at 450 – 500 nm. The red-shifting of the respective spectral irradiances were proven to have a positive improvement in the organic solar cells' performance, especially under illumination of local diffuse spectral irradiance. The calculated *ISI* values for total average, total direct, and also total diffuse are 408.36 W/m^2, 596.81 W/m^2, and 156.72 W/m^2 respectively. The performance of each organic material was studied through the curve fitting method conducted to the device quantum efficiency in order to calculate relevant photovoltaic data that required for power conversion efficiency (*PCE*) calculations. Among the 5 studied organic materials' groups, [PTB7: $PC_{60}BM$] appeared to be the best organic materials for the designation of organic solar cells, by having the *PCE* of 6.90%, and also having the greatest percentage improvement (10.10%) under local total average spectral irradiance. In addition to spectrum analysis on local spectral irradiances, the analysis local average photon energy (*APE*) was also conducted, with the average *APE* index calculated for local direct spectral irradiance,

local diffuse spectral irradiance, and local total average spectral irradiance are 1.65 eV, 1.75 eV, and 1.69 eV respectively.

For future works, a few more sets of organic material combinations should be studied in order to maximise the knowledge about the current available organic materials that the market have so that more options of the materials can be considered. The architecture of the organic solar cells (*OSCs*) should also be considered as one of the selection parameters because based on literature review, it shows that the lifetime of the *OSCs* is mainly depends on its device architecture. Upon successfully selected and fabricated out organic solar cells, it is advisable to conduct an on-site evaluation for the *OSCs*' performance under various local spectral irradiances in order to obtain more practical results. An optimisation of the selected organic materials may also be conducted to maximise the performance potential that an organic material may have. This can be done by studying the morphology of the relevant materials' surface, physical and chemical characteristics of the materials, in order to have better understanding about the materials.

REFERENCES

Brus, V.V. "Light Dependent Open-Circuit Voltage of Organic Bulk Heterojunction Solar Cells In The Presence Of Surface Recombination". *Organic Electronics* 29 (2016): 1-6.

Chong, Kok-Keong et al. "Comprehensive Method for Analyzing the Power Conversion Efficiency of Organic Solar Cells under Different Spectral Irradiances Considering both Photonic and Electrical Characteristics". *Applied Energy* 180 (2016): 516-523.

Cornaro, Cristina and Angelo Andreotti. "Influence of Average Photon Energy Index on Solar Irradiance Characteristics and Outdoor Performance of Photovoltaic Modules". *Prog. Photovolt: Res. Appl.* (2012).

"Defining Standard Spectra for Solar Panels". Greenrhinoenergy.com. Web. 4 Aug. 2016.

Fan, Ling et al. "A New Two-Dimensional Donor/Acceptor Copolymer Based On 4,8-Bis(2′-Ethylhexylthiophene)Thieno[2,3-F]Benzofuran For High-Performance Polymer Solar Cells".*Journal of Materials Chemistry C* 2.28 (2014): 5651.

Foster, J. M., J. Kirkpatrick, and G. Richardson. "Asymptotic And Numerical Prediction Of Current-Voltage Curves For An Organic Bilayer Solar Cell Under Varying Illumination And Comparison To The Shockley Equivalent Circuit". *J. Appl. Phys.* 114.10 (2013): 104501.

"General Climate of Malaysia". Met.gov.my. 2016. Web. 3 Aug. 2016.

Guechi, A., M. Chegaar, and M. Aillerie. "Air Mass Effect on the Performance of Organic Solar Cells". *Energy Procedia* 36 (2013): 714-721.

"Introduction to Solar Radiation". Newport.com. Web. 3 Aug. 2016.

Kasap, S. O. *Optoelectronics and Photonics*. Upper Saddle River, NJ: Prentice Hall, 2001. Print.

Kazem, H.A. et al. "Effect of Humidity on the PV Performance in Oman". *Asian Transactions on Engineering* 02.04 (2012): 29 - 32.

Lim, Fang Jeng et al. "Influence Of A Novel Fluorosurfactant Modified PEDOT:PSS Hole Transport Layer On The Performance Of Inverted Organic Solar Cells". *Journal of Materials Chemistry*22.48 (2012): 25057.

Lin, Rui et al. "Enhancement of Ternary Blend Organic Solar Cell Efficiency Using PTB7 as A Sensitizer". *Synthetic Metals* 192 (2014): 113-118.

Liu, Jiangang et al. "Improving The Morphology Of PCDTBT:PC70BM Bulk Heterojunction By Mixed-Solvent Vapour-Assisted Imprinting: Inhibiting Intercalation, Optimizing Vertical Phase Separation, And Enhancing Photon Absorption". *J. Phys. Chem. C* 118.9 (2014): 4585-4595.

Liu, Yuhang et al. "Aggregation and Morphology Control Enables Multiple Cases of High-Efficiency Polymer Solar Cells". *Nature Communications* 5 (2014): 5293.

Madsen, Morten. "Why Do Polymer Solar Cells Degrade". Plasticphotovoltaics.org. Web. 4 Aug. 2016.

Mat Desa, M.K. et al. "Silicon Back Contact Solar Cell Configuration: A Pathway Towards Higher Efficiency". Renewable and Sustainable Energy Reviews 60 (2016): 1516-1532.

Mambrini, Thomas et al. "Photovoltaic Yield: Correction Method for the Mismatch between the Solar Spectrum and the Reference ASTMG AM1.5G Spectrum". *EPJ Photovolt.* 6 (2015): 60701.

McGinley, Mark. "Climate 0f Malaysia". eoearth.org. 2016. Web. 2 Apr. 2016.

"Meteorological Data". Fao.org. 2016. Web. 13 Aug. 2016.

Mekhilef, S. et al. "Solar Energy In Malaysia: Current State And Prospects". *Renewable and Sustainable Energy Reviews* 16.1 (2012): 386-396.

Morinaka, Yuta et al. "Synthesis and Photovoltaic Properties of Acceptor Materials Based On the Dimerization of Fullerene C60 for Use in Efficient Polymer Solar Cells". *Chemical Communications* 49.35 (2013): 3670.

Nann, Stefan and Carol Riordan. "Solar Spectral Irradiance under Clear and Cloudy Skies: Measurements and a Semiempirical Model". *Journal of Applied Meteorology* 30.4 (1991): 447-462.

Nofuentes, G. et al. "Analysis of the Dependence of the Spectral Factor of Some PV Technologies on the Solar Spectrum Distribution". *Applied Energy* 113 (2014): 302-309.

Norton, M., A.M. Gracia Amillo, and R. Galleano. "Comparison of Solar Spectral Irradiance Measurements Using the Average Photon Energy Parameter". *Solar Energy* 120 (2015): 337-344.

"Organic Solar Power". I-sis.org.uk. 2006. Web. 12 Aug. 2016.

Savenije, Tom J. "Organic Solar Cells". Solar Cells. Rene Janssen. 1st ed. 2014. 8.14. Web. 19 Aug. 2016.

"Sepang-KL International Airport, Malaysia". Wunderground.com. 2016. Web. 3 Aug. 2016.

Shockley, William and Hans J. Queisser. "Detailed Balance Limit of Efficiency Of P-N Junction Solar Cells". *J. Appl. Phys.* 32.3 (1961): 510.

Shwartz, Mark. "Perovskites Provide Big Boost to Silicon Solar Cells, Stanford Study Finds Energy". *Energy.stanford.edu*. 2016. Web. 15 Aug. 2016.

Sirisamphanwong, C. et al. "Average Photon Energy under Thailand's Climatic Condition". *Internation Journal of Renewable Energy* 6.1 (2016): 25-29.

Sirisamphanwong, Chattariya, Nipon Ketjoy, and Chatchai Sirisamphanwong. "The Effect of Average Photon Energy and Module Temperature on Performance of Photovoltaic Module under Thailand's Climate Condition". *Energy Procedia* 56 (2014): 359-366.

Tanenbaum, David M. et al. "Edge Sealing for Low Cost Stability Enhancement of Roll-To-Roll Processed Flexible Polymer Solar Cell Modules". Solar Energy Materials and Solar Cells 97 (2012): 157-163.

Us, About and Mathias Maehlum. "Which Solar Panel Type Is Best? Mono-, Polycrystalline Or Thin Film?". Energy Informative. 2015.

U.S. Standard Atmosphere, 1976. Washington D.C: National Oceanic and Atmospheric Administration National Aeronautics and Space Administration United States Air Force, 1976.

Varikoden, H., et al. Seasonal variation of rainfall characteristics in different intensity classes over Peninsular Malaysia. J. Hydrol. (2011), doi:10.1016/j.jhydrol.2011.04.021

Wang, Kai et al. "Inverted Organic Photovoltaic Cells". Chem. Soc. Rev. 45.10 (2016): 2937-2975.

Würfel, Uli et al. "Impact of Charge Transport on Current–Voltage Characteristics and Power-Conversion Efficiency of Organic Solar Cells". Nature Communications 6 (2015): 6951.

APPENDICES

APPENDIX A: TABLES

Table A.1: Weightage for Specific Wavelength Range for each Hour under the Illumination of Local Direct Spectral Irradiance (the cells' values that have weightage more than 0.80 will be yellow-coloured, which is used to compare the shift of the spectral irradiance of each hour)

Wavelength range (nm)	**Weightage for Specific Wavelength Range**				
	0830	**0930**	**1030**	**1130**	**1230**
300 – 350	0.09	0.13	0.16	0.17	0.18
350 – 400	0.28	0.38	0.45	0.48	0.49
400 – 450	0.57	0.71	0.77	0.80	0.81
450 – 500	0.79	0.89	0.94	0.95	0.95
500 – 550	0.91	0.96	0.98	0.99	0.98
550 – 600	0.99	1.00	1.00	1.00	1.00
600 – 650	1.00	0.97	0.95	0.94	0.94
650 – 700	0.92	0.86	0.83	0.82	0.82
700 – 750	0.96	0.85	0.80	0.78	0.78
750 – 800	0.96	0.81	0.75	0.72	0.73
800 – 850	0.81	0.67	0.61	0.59	0.59
850 – 900	0.61	0.50	0.46	0.45	0.45
900 – 950	0.23	0.21	0.20	0.21	0.21
950 – 1000	0.36	0.28	0.24	0.23	0.23
1000 – 1050	0.62	0.45	0.39	0.36	0.35
1050 – 1100	0.37	0.28	0.25	0.24	0.24

Table A.2: Weightage for Specific Wavelength Range for each Hour under the Illumination of Local Direct Spectral Irradiance (the cells' values that have weightage more than 0.80 will be yellow-coloured, which is used to compare the shift of the spectral irradiance of each hour)

Wavelength range (nm)	**Weightage for Specific Wavelength Range**				
	1330	**1430**	**1530**	**1630**	**1730**
300 – 350	0.18	0.18	0.16	0.13	0.11
350 – 400	0.49	0.49	0.45	0.39	0.34
400 – 450	0.80	0.80	0.76	0.70	0.64
450 – 500	0.95	0.95	0.92	0.88	0.84
500 – 550	0.98	0.99	0.97	0.95	0.94
550 – 600	1.00	1.00	1.00	1.00	1.00
600 – 650	0.94	0.94	0.96	0.97	0.99
650 – 700	0.83	0.82	0.85	0.87	0.91
700 – 750	0.79	0.78	0.83	0.87	0.92
750 – 800	0.73	0.73	0.78	0.83	0.90
800 – 850	0.59	0.59	0.64	0.69	0.76
850 – 900	0.45	0.45	0.49	0.52	0.57
900 – 950	0.22	0.22	0.23	0.24	0.24
950 – 1000	0.23	0.23	0.26	0.28	0.32
1000 – 1050	0.35	0.34	0.40	0.45	0.53
1050 – 1100	0.24	0.23	0.25	0.29	0.31

APPENDIX B: PUBLICATION

Applied Energy 180 (2016) 516–523

Contents lists available at ScienceDirect

Applied Energy

journal homepage: www.elsevier.com/locate/apenergy

Comprehensive method for analyzing the power conversion efficiency of organic solar cells under different spectral irradiances considering both photonic and electrical characteristics

Kok-Keong Chong [a,b,*], Petr P. Khlyabich [b], Kai-Jeat Hong [a], Marcos Reyes-Martinez [b], Barry P. Rand [c], Yueh-Lin Loo [b]

[a] Lee Kong Chian Faculty of Engineering and Science, Universiti Tunku Abdul Rahman, Bandar Sungai Long, 43000 Kajang, Selangor, Malaysia
[b] Department of Chemical and Biological Engineering, Princeton University, Princeton, NJ, USA
[c] Department of Electrical Engineering and Andlinger Center for Energy and the Environment, Princeton University, Princeton, NJ, USA

HIGHLIGHTS

- Method to analyze power-conversion efficiency under various solar irradiance.
- Power-conversion efficiency at local irradiance is 5.4% higher than AM1.5G.
- Diffuse local irradiance has gain of 23.7–27.9% relative to AM1.5G conditions.
- Annual average energy density yield is estimated as 31.89 kW h/m^2 in Malaysia.

GRAPHICAL ABSTRACT

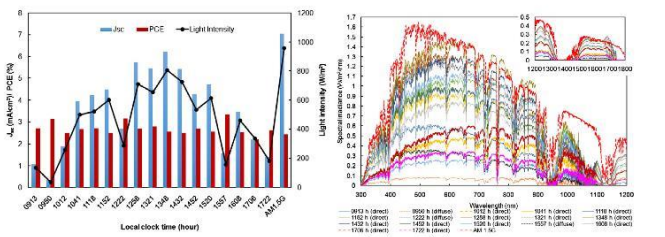

ARTICLE INFO

Article history:
Received 22 December 2015
Received in revised form 11 July 2016
Accepted 1 August 2016

Keywords:
Organic solar cell
AM1.5G
Poly(3-hexylthiophene):phenyl-C_{61}-butyric acid methyl ester
Power conversion efficiency
Spectral variation
Local solar irradiance

ABSTRACT

The solar spectral irradiance varies significantly for different locations and time due to latitude, humidity, cosine effect of incident sunlight, etc. For convenience, the power-conversion efficiency of a solar cell is referenced to the international standard of AM1.5G spectral irradiance, which inevitably leads to varying performance of deployed solar cells under the specific local climate and insolation conditions. To predict the actual performance of solar cells under local climate conditions, we propose a methodology to compute the power-conversion efficiency of organic photovoltaic cells based upon indoor measurement with a solar simulator, the measured local solar spectrum, and making use of both optical and electrical factors. From our study, the annual average energy density yield of poly(3-hexylthiophene):phenyl-C_{61}-butyric acid methyl ester (P3HT:PCBM) bulk-heterojunction organic solar cells under the local spectral irradiance of Malaysia is estimated to be 31.89 kW h/m^2 and the power-conversion efficiency is increased by 5.4% compared to that measured under AM1.5G conditions. In addition, diffuse solar irradiance (cloudy condition) was found to be in favor of P3HT:PCBM solar cells, with gain of 23.7–27.9% relative to AM1.5G conditions.

© 2016 Elsevier Ltd. All rights reserved.

1. Introduction

The demand for solar photovoltaic (PV) systems has increased dramatically for the last several decades as a source of renewable energy to reduce the use of fossil fuels [1]. To that end, the search

* Corresponding author at: Lee Kong Chian Faculty of Engineering and Science, Universiti Tunku Abdul Rahman, Bandar Sungai Long, 43000 Kajang, Selangor, Malaysia.
E-mail addresses: chongkk@utar.edu.my, kokkeong_c@yahoo.com (K.-K. Chong).

http://dx.doi.org/10.1016/j.apenergy.2016.08.002
0306-2619/© 2016 Elsevier Ltd. All rights reserved.

Figure A 1: Comprehensive method for analysing the *PCE* of *OSCs* under different spectral irradiances considering both photonic and electrical characteristics (page 1)

for high efficiency solar cells with low-cost fabrication has intensified research in both inorganic and organic PV devices [2]. Currently, inorganic PV devices, e.g. silicon (Si), III–V semiconductors, cadmium telluride (CdTe), copper indium gallium selenide (CIGS), etc., are commercial technologies. Due to various advantages, such as high power-conversion efficiency (PCE), stability, and being a mature technology, Si solar cells dominate the overall market, but do have drawbacks of being rigid and heavy, making them difficult for applications that demand lower weight. For this, thin-film solar cell technology is better suited with CdTe based PV currently the market leader, although with notable issues regarding material scarcity and toxicity.

With the use of conjugated organic materials such as polymers, thin film solar cells can be made flexible and with a myriad of colors [3]. The potential applications of organic solar cells are diverse, ranging from flexible solar modules and semitransparent solar cells in windows, to building and mobile applications [4]. Solar cells based on organic materials can be fabricated using solution processing, employing various coating, printing, and roll-to-roll techniques, which could lower manufacturing costs by avoiding high temperature and vacuum processes [5]. Furthermore, organic semiconductors have high absorption coefficients that allow very thin films to be used. The last five years have seen significant progress for this technology. To date, the highest reported PCE for a thin film organic solar cell (OSC) with an active area of 0.0429 cm^2 is 11.5% and a mini-module organic solar device with active area of 26.14 cm^2 is 9.7% [6]. The major challenge for the organic photovoltaics (OPV) community is to deliver high performance combined with sufficient long-term stability. Considering the advantages and significantly increased efficiencies of organic solar cells, OPV products are increasingly being used in solar panels on books, bags, and windows, etc. For reasons of standardization, the AM1.5G solar spectrum is used as the universal reference to compare the PCE of all PV modules. Yet, the local spectral irradiance can be quite different from that of AM1.5G depending on the latitude, humidity, cosine effect of incident sunlight, etc. Although organic semiconductors often possess high absorption coefficients ($\sim 10^5$ cm^{-1}), their absorption tends to occur in relatively narrow bands as compared to inorganic solar cells and thus are very sensitive to changes in the spectral irradiance.

The influence of varying spectral irradiance on the performance of solar cells is well known by the international community conducting work in this area. To date, the impact of different spectral irradiances on outdoor performance of PV modules are assessed based on two widely used parameters: the average photon energy (APE) and the spectral mismatch factor (SMF). The APE is calculated by dividing the integrated irradiance by the integrated photon flux density, yielding an average energy per photon (eV). As such, APE is a useful parameter that can represent the extent to which a spectrum shifts relative to AM1.5 towards either the red or the blue. A large value of APE corresponds to a spectrum enriched in blue light whereas a small value indicates a spectrum that is enriched in red light [7]. The SMF is the energetic gain or loss in effective irradiance available to a specific PV technology compared to the total broadband irradiation measured by a pyranometer, and compared to the theoretical case of a permanent reference spectral irradiance [8]. Hence, SMF greater than one means that the actual solar spectral distribution is producing lower short-circuit current as compared to that of AM1.5G and indicates spectral losses. Accordingly, an SMF less than one indicates spectral gain [9]. In 2003, Betts et al. studied the effect of variations of spectral irradiance outdoors on single-, double-, and triple-junction amorphous silicon solar cells and utilized APE as a parameter. They found that there was only a small variation in both the fill factor and open-circuit voltage as a function of APE [10]. In their study, all devices showed a general increase in PCE with APE whereas the response of the single-junction amorphous Si device was virtually linear with APE. To date, many investigations have probed the effect of having a spectral irradiance distribution under outdoor conditions for different types of PV modules, e.g., amorphous or crystalline silicon, etc., deployed in Japan [11–14], Thailand [15], Italy [7], Germany [8,16], UK [10,17], Spain [9] indexed by APE and SMF. The performance ratio (PR) as a function of SMF and module temperature was employed as an indicator of the PV performance; it is defined as the actual output energy divided by the nominal output energy calculated under standard test condition for a comparison with APE [9,12]. Recently, Moreno-Sáez and Mora-López modeled the distribution of solar spectral irradiance based on data mining techniques and proposed to use APE as a parameter for characterizing the solar spectral distribution [18]. The use of both APE and SMF have been carried out extensively on commercially available cells [8,9] as well as emerging thin-film perovskite solar cells [19]. While commonly employed to characterize devices, these aforementioned parameters, including APE, SMF, PR, do not absolutely or precisely quantify the performance of specific PV technologies. Instead, they provide relative comparisons to reveal which PV technology is favorable under specific spectral irradiance.

To predict the performance of organic solar cells under local spectral irradiance, we require both a photonic component (photocurrent or short-circuit current density, J_{sc}, derived from the spectral irradiance and external quantum efficiency, EQE) and electrical components of a PV device (fill factor, FF, and open-circuit voltage, V_{oc}) to compute PCE. However, some solar-cell technologies cannot be modeled with the assumption of invariant FF and V_{oc} as a function of J_{sc}. Thus, to determine PCE, we not only need to know the spectral irradiance and EQE but also require the electrical characteristics of a PV device in order to obtain a relationship between FF, V_{oc} and J_{sc}. In this study, we propose a comprehensive methodology to study the impact of local spectral irradiance, and we have conducted this analysis using an organic solar cell as an example. For this purpose, we have acquired the local solar spectra via random data collection and accumulation throughout the year from July 2015 to June 2016 with local clock time 0800–1800 h at Universiti Tunku Abdul Rahman, Bandar Sungai Long, Malaysia (latitude 3.0408°N, longitude 101.7942°E) as a case study. The solar spectral irradiances are reported in three ways: an average spectrum that encompasses the mean of all spectra, an average diffuse spectrum that only includes diffuse spectra and an average direct spectrum that only includes direct spectra. An OPV cell with an active area of 1 cm^2 was characterized indoors to ascertain the electrical properties' change with incident light. By using the local irradiance data and electrical characteristics of the OPV device, we have estimated the PCE under local spectral irradiances and the annual energy yield of the OPV device in a city in Malaysia before the actual photovoltaic device would be delivered and installed at the site. Additionally, this approach may also be used to provide guidelines for selecting the most appropriate organic photoabsorbers for the solar device whose optical properties match well with the local spectral irradiance in order to maximize the annual energy yield.

2. Methodology

To analyze the PCE of organic solar cells under different spectral irradiances, we have formulated a detailed methodology based on experimental results and a computational algorithm. The study is important to understand the PCE for various types of photovoltaic devices, and here demonstrated for organic solar cells, under different spectral irradiances. In particular, the use of this approach

Figure A 2: Comprehensive method for analysing the *PCE* of *OSCs* under different spectral irradiances considering both photonic and electrical characteristics (page 2)

eliminates the need to manufacture and deploy a photovoltaic module followed by on-site data collection.

In the proposed methodology, shown in Fig. 1, the first step is to obtain the electrical characteristics of organic solar cells based on laboratory test conditions including the relationship between V_{oc} and J_{sc}, the relationship between FF and J_{sc}, and spectral response. Secondly, on-site measurement is conducted to acquire the local solar irradiance using a spectrometer. Finally, the computational method is employed to determine the PCE of solar cells.

The FF and PCE can be calculated using the following formulas

$$\mathrm{FF} = \frac{J_{\max} V_{\max}}{J_{sc} V_{oc}} \quad (1)$$

$$\mathrm{PCE} = \frac{\mathrm{FF} \times J_{sc} V_{oc}}{P_{in}/A} \quad (2)$$

where $J_{\max}$ (mA/cm^2) and $V_{\max}$ (V) are the current density and voltage at the maximum power point, respectively; P_{in}/A is the incident light intensity with unit mW/cm^2 in which P_{in} is power of incident light in unit mW and A is the corresponding area (cm^2).

The generalized Shockley equation that describes the relationship between current density (J) and voltage (V) of organic solar cells is well established [20–23]

$$J = \frac{R_p}{R_s + R_p}\left\{J_s\left[\exp\left(\frac{e(V - JR_s)}{nkT}\right) - 1\right] + \frac{V}{R_p}\right\} - J_{ph}(V) \quad (3)$$

where R_p is the parallel resistance, R_s is the series resistance, J_s is the saturation current density, e is electron charge, n is the diode ideality factor, k is Boltzmann constant, and $J_{ph}(V)$ is the voltage dependent photocurrent density.

For solar cells with minimal leakage current, Eq. (3) can be simplified to

$$J = J_s\left[\exp\left(\frac{e(V - JR_s)}{nkT}\right) - 1\right] - J_{ph}(V) \quad (4)$$

The first term corresponds to thermally generated current dominated by recombination at the donor/acceptor interface, and the second term accounts for photo-generated current [23].

At open-circuit conditions ($J = 0$, $V = V_{oc}$), the rate of carrier recombination equals the rate of optical carrier generation. Assuming open-circuit conditions, a short-circuit current of $J_{sc} = J_{ph}(0) \gg J_s$, and a low series resistance, Eq. (4) can be further solved to obtain the following:

$$V_{oc} \approx \frac{nkT}{e} \ln\left(\frac{J_{sc}}{J_s}\right) \quad (5)$$

Since J_{sc} is linearly proportional to illumination, we can obtain the graph of V_{oc} versus J_{sc} by changing the light intensity of solar simulator. From Eq. (5), Eq. (6) follows provided that a set of values (J_{sc1}, V_{oc1}) is obtained from the plotted V_{oc} versus J_{sc} graph.

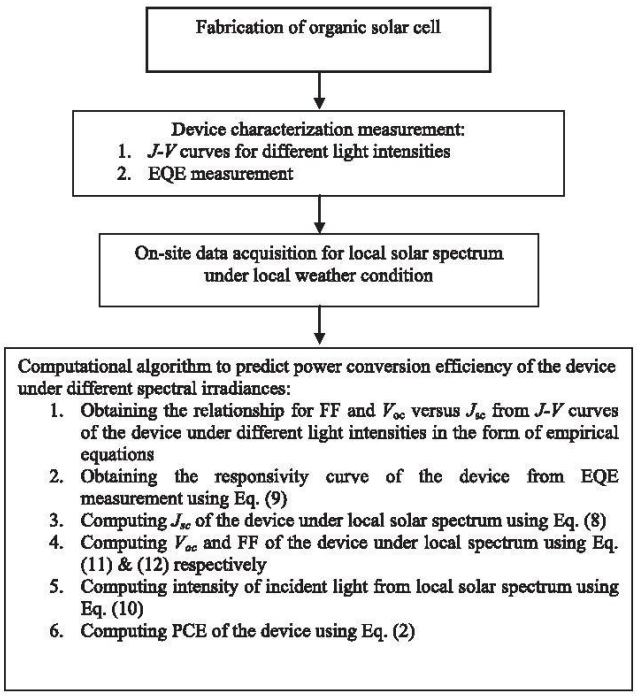

Fig. 1. Flow chart to show the detailed methodology to compute power conversion efficiency of an organic solar cell based on the local solar spectrum and device characteristic curves.

Figure A 3: Comprehensive method for analysing the *PCE* of *OSCs* under different spectral irradiances considering both photonic and electrical characteristics (page 3)

$$V_{oc} - V_{oc1} = \frac{nkT}{e}\ln\left(\frac{J_{sc}}{J_s}\right) - \frac{nkT}{e}\ln\left(\frac{J_{sc1}}{J_s}\right) \quad (6)$$

$$V_{oc} = \frac{nkT}{e}\ln(J_{sc}) + \left[V_{oc1} - \frac{nkT}{e}\ln(J_{sc1})\right] \quad (7)$$

The current density of an organic solar cell can be calculated using the following equation:

$$J_{sc} = \int_{\lambda_1}^{\lambda_2} S_L(\lambda)\cdot R(\lambda)\mathrm{d}\lambda \quad (8)$$

λ_1 and λ_2 are lower limit and upper limit wavelengths of incident light respectively, $S_L(\lambda)$ is spectral irradiance of local spectrum and $R(\lambda)$ is the spectral responsivity of the device.

$$R(\lambda) = \frac{e\lambda}{hc}\eta_{EQE}(\lambda) \quad (9)$$

where η_{EQE} is external quantum efficiency of the device, λ is wavelength of incidence light, h is Planck's constant, c is the speed of light.

Incident light intensity can be calculated as following

$$P_{in}/A = \int_{\lambda_1}^{\lambda_2} S_L(\lambda)\mathrm{d}\lambda \quad (10)$$

2.1. Device fabrication

In the structure of the organic solar cell used in this work, PEDOT:PSS (3,4 polyethylenedioxythophene polystyrenesulfonate) from Heraeus Clevios PH 500 was used as the hole injection layer. The active layer was made up of a mixture of P3HT (poly-3-hexylthiophene-2,5-diyl with purity) with purity of 99.9% (Sigma-Aldrich) and PCBM (phenyl-C_{61}-butyric acid methyl ester) with purity >99.0%, (American Dye Source) in a 1:0.8 wt proportion. The solid powders of P3HT and PCBM were added separately to chlorobenzene solution (purity 99.8%, Sigma Aldrich) at a proportion of 20 mg/mL and stirred for five hours. The device structure is: glass/indium tin oxide (ITO)/PEDOT:PSS (40 nm)/P3HT:PCBM (100 nm)/Al (100 nm).

The ITO-coated glass substrates (Thin Film Devices) were cleaned consecutively in the following solutions: deionized water (10 min), acetone (5 min) and isopropyl alcohol (5 min) in ultrasonic bath. The PEDOT:PSS solution was filtered with 0.45-μm sterile polyvinylidene fluoride (PVDF) membrane filter and spin-coated onto the cleaned substrate at 4000 rpm for 40 s. Then, the coated substrate was baked and dried at 120 °C for 30 min to remove residual water. Active layer was deposited by spin coating at 900 rpm for 60 s, which was filtered with a 0.45-μm polytetrafluorethylene (PTFE) membrane filter. Finally, the 100 nm thick aluminum electrode was deposited at a background pressure of 3×10^{-6} mbar and the device stack was subsequently annealed at 150 °C for 30 min. The device area was 1 cm^2.

2.2. Device characterization measurement

All measurements, except external quantum efficiency (EQE), were performed under inert N_2 atmosphere. The measured and integrated currents were similar, indicating proper lamp calibration and sufficient stability of the devices during testing. After the fabrication of device, the current density vs. voltage (*J-V*) curves were measured by a Keithley 2635A source measure unit. The photocurrent was measured under AM1.5G illumination at 100 mW/cm^2 using a Newport solar simulator model 6258 (300 W Xenon lamp ozone-free) and a Si reference cell traceable to Newport was used to calibrate light intensity. The illumination intensity of the solar simulator was changed by applying a Spiricon optical filter wheel with operational wavelength ranging from 400 nm to 2600 nm. Furthermore, an EQE measurement system from Oriel Instruments, Newport was employed to measure EQE.

2.3. Solar spectrum acquisition

To study the effect of local solar irradiance as compared to AM1.5G spectral irradiance, we used the location in the campus area of Universiti Tunku Abdul Rahman (UTAR), Bandar Sungai Long, Malaysia (latitude 3.0408°N, longitude 101.7942°E). For acquiring full solar spectrum to cover the wavelengths ranging from 300 nm to 1800 nm, we employed a configuration of combined two types Avantes spectrometers comprised of AvaSpec-2048-USB2-RM (bandwidth: 200–1100 nm) and AvaSpec-NIR256-1.7-RM (1000–2000 nm). For data acquisition, the solar spectral irradiances were collected from July 2015 to June 2016 for local clock time from 0800 to 1800 h at intervals of 10 min per capture during which the spectrometer sensor was always pointed towards the sun. There are two parts to the analysis. First, we selected a mostly sunny day on July 13, 2015 and local time from 0913 h to 1722 h to assess how the solar spectrum varies across the day. Secondly, we performed averaging on the randomly selected solar spectral irradiances throughout the year in three categories: annual average diffuse spectra, annual average direct spectra, and annual average total spectra (including both direct and diffuse spectra).

3. Result and discussion

The organic solar cell was measured at different light intensities ranging from 15 to 100 mW/cm^2 as shown in Fig. 2. As expected, both photocurrent and photovoltage increase as a function of increasing incident light intensity.

The relationship between V_{oc} and J_{sc} is investigated by extracting their values under different light intensities, as shown in Fig. 3. The empirical formula of V_{oc} vs. J_{sc} plot obtained via curve fitting is provided in Eq. (11) and matches well with that expected from the Shockley equation in Eq. (7):

$$V_{oc} = 0.0354\ln(J_{sc}) + 0.5528 \quad (11)$$

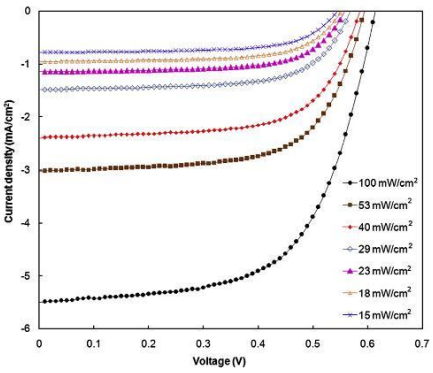

Fig. 2. *J-V* curves for a P3HT:PCBM device under different intensities of a solar simulator, specifically 15 mW/cm^2, 18 mW/cm^2, 23 mW/cm^2, 29 mW/cm^2, 40 mW/cm^2, 53 mW/cm^2 and 100 mW/cm^2.

Figure A 4: Comprehensive method for analysing the *PCE* of *OSCs* under different spectral irradiances considering both photonic and electrical characteristics (page 4)

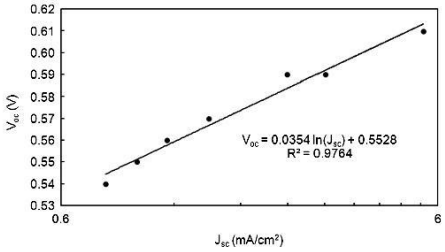

Fig. 3. The relationship between open circuit voltage (V_{oc}) and short-circuit current density (J_{sc}) of organic solar cells under different irradiances as extracted from the *J-V* characteristic plots.

By comparing Eqs. (7) and (11) at room temperature (298.15 K), the diode ideality factor, *n*, of the P3HT:PCBM device can be calculated as

$$\textbf{Ideality factor},\ n = \frac{0.0354 \times 1.602 \times 10^{-19}\ \text{C}}{298.15\ \text{K} \times 1.38 \times 10^{-23}\ \text{J K}^{-1}} = 1.378$$

This value is reasonably close to the value reported by Foertig et al. who also obtained an ideality factor for P3HT:PCBM solar cells of 1.21 [20].

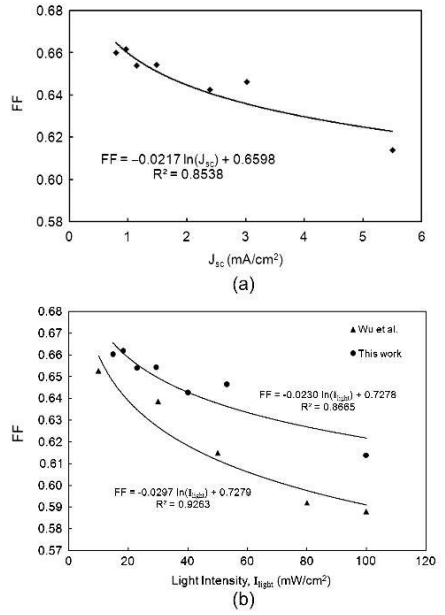

Fig. 4. (a) The relationship between fill factor (FF) and short circuit current density (J_{sc}) of organic solar cells under different irradiances as extracted from the *J-V* characteristic plots. (b) A comparison graph of fill factor (FF) versus light intensity between this work and the data provided by Wu et al. [26].

Furthermore, the relationship between FF and J_{sc} for the organic solar cell under different light intensities were also extracted as shown in Fig. 4(a). According to the observations of Jin et al. and Yoo et al., the FF vs. J_{sc} curve should behave as a logarithmic function [24,25]. Unlike the well-known relationship between V_{oc} and J_{sc} that can be derived by the Shockley equation, an analytical formula to relate FF and J_{sc} (light intensity) is complicated by the voltage dependent photocurrent. From the work by Wu et al., they found that the FF of a P3HT:PCBM solar cell decreased with light intensity and was attributed to two main parameters: (i) light intensity induced parallel resistance; and (ii) more significant bimolecular recombination [26]. For verification of the relationship between FF and J_{sc} (proportional to light intensity), we plot a comparison graph between the data provided by Wu et al. and our data for FF versus light intensity in Fig. 4(b); both curves show a similar functional form; we also obtained comparable constants. The empirical formula of FF versus J_{sc} plot can be expressed in the following equation:

$$\text{FF} = -0.0217 \ln(J_{sc}) + 0.6598 \quad (12)$$

Finally, the EQE and spectral responsivity curves of the fabricated P3HT:PCBM solar device are displayed in Fig. 5. The spectral responsivity curve was derived from the EQE curve using Eq. (9).

The PCE of fabricated P3HT:PCBM was measured as 2.04% with FF of 0.61 under AM1.5G illumination at 100 mW/cm^2, which is considered acceptable for larger device with active area of 1 cm^2. According to Jin et al., they have shown that PCE of P3HT:PCBM solar device is decreased when the active area is increased in which PCE = 2.0–2.1% and FF = 63.6–66% for active area of 0.2 cm^2 whereas PCE = 1.6–1.9% and FF = 54.4–57.1% for active area of 25 cm^2 [27].

For the first part of study, we analyzed the effect of different spectral irradiances on the PCE of P3HT:PCBM solar device. Fig. 6 shows the local solar spectral irradiance measured at different local times from 0913 h (morning) to 1722 h (late afternoon) on 15th July 2016. From Fig. 6, we can divide the local spectra into two sections: (a) the range of 300–1200 nm (main plot) is significant to the power conversion because organic solar cells are photoactive in this range of wavelengths; (b) the range of 1200–1800 nm (inset with the same definition in both axes) is important to calculate the total input power from the sunlight in the PCE computation. The standard AM1.5G spectrum is also included for comparison. In the local spectral irradiance, there were three moments when the sky was cloudy, labeled as diffuse in the spectral irradiance plots, at 0950 h, 1222 h, and 1557 h. Moreover, there is a significant red shift in the local spectral irradiance observed at 1012 h, 1706 h, 1722 h, which are further

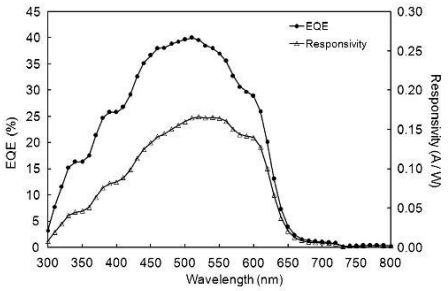

Fig. 5. External quantum efficiency (EQE) and responsivity of the P3HT:PCBM solar cell.

Figure A 5: Comprehensive method for analysing the *PCE* of *OSCs* under different spectral irradiances considering both photonic and electrical characteristics (page 5)

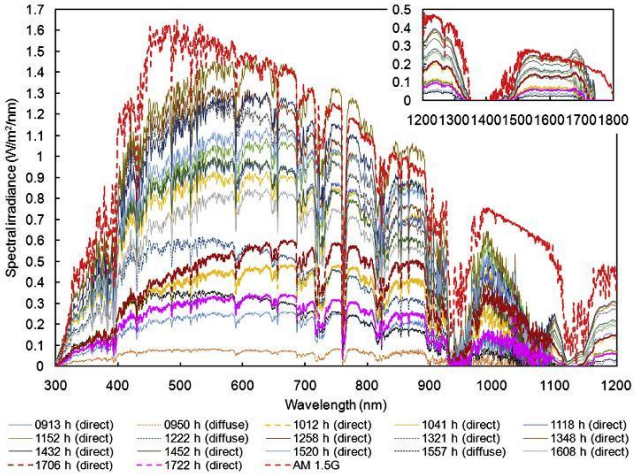

Fig. 6. Spectral irradiance of AM1.5G and local spectrum at different local clock time from 0913 h (morning) to 1722 h (late afternoon).

Table 1
The computed values for J_{sc}, V_{oc}, FF, light intensity, PCE, and gain for spectral irradiance of different local clock time from 0913 h to 1722 h as well as AM1.5G for comparison.

Local clock time	J_{sc} (mA/cm^2)	V_{oc} (V)	FF	Light intensity (W/m^2)	PCE (%)	Gain (%)
0913 h (direct)	0.78	0.54	0.67	137	2.07	1.4
0950 h (diffuse)	0.26	0.50	0.69	39	2.29	12.1
1012 h (direct)	1.38	0.56	0.65	261	1.94	−4.8
1041 h (direct)	2.87	0.59	0.64	501	2.16	5.6
1118 h (direct)	3.07	0.59	0.64	524	2.20	7.9
1152 h (direct)	3.25	0.59	0.63	603	2.03	−0.5
1222 h (diffuse)	1.95	0.58	0.65	288	2.53	23.7
1258 h (direct)	4.17	0.60	0.63	711	2.22	8.9
1321 h (direct)	3.96	0.60	0.63	655	2.29	12.2
1348 h (direct)	4.49	0.61	0.63	807	2.11	3.6
1432 h (direct)	3.92	0.60	0.63	725	2.05	0.4
1452 h (direct)	3.10	0.59	0.63	535	2.18	7.0
1520 h (direct)	3.42	0.60	0.63	617	2.09	2.4
1557 h (diffuse)	1.15	0.56	0.66	161	2.61	27.9
1608 h (direct)	2.51	0.59	0.64	461	2.04	−0.3
1706 h (direct)	1.58	0.57	0.65	339	1.72	−15.5
1722 h (direct)	1.01	0.55	0.66	183	2.02	−1.2
AM1.5G	5.14	0.61	0.62	960	2.04	–

highlighted in dotted line with colors orange, maroon and pink respectively.

Based on the computational algorithm detailed in Fig. 1, we can obtain the values of J_{sc}, V_{oc}, FF, light intensity and PCE for the cases of the AM1.5G spectrum as well as the local spectral irradiances from 0913 h to 1722 h as shown in Table 1. In Fig. 7, we plotted three major parameters, i.e. J_{sc}, PCE and light intensity, to provide a clear picture on the daily variation of incident solar flux and the annual energy yield of organic solar device. Except cloudy moments at 0950 h, 1222 h, and 1557 h, the distribution of light intensity (spectral irradiance) and the corresponding photocurrent output (J_{sc}) have shown normal Gaussian pattern with peak near to solar noon for the local site location at 3.04°N, 101.79°E (standard time zone is 120°E). However, the PCE does not vary proportionally with the light intensity and photocurrent output because FF behaves in the opposite manner (inversely proportional to J_{sc}) as revealed in Fig. 4.

At the same time, we also made a comparison of PCE for our fabricated P3HT:PCBM device operating under the local spectral irradiances relative to the AM1.5G spectrum by defining the following new parameter:

$$\text{Gain} = 100\% \times (\text{PCE}_{\text{LSI}} - \text{PCE}_{\text{AM1.5G}})/\text{PCE}_{\text{AM1.5G}} \quad (13)$$

where PCE_{LSI} and $\text{PCE}_{\text{AM1.5G}}$ are the power-conversion efficiencies at local spectral irradiances in Malaysia and standard irradiance AM1.5G conditions, respectively.

From the simulated result in Table 1, most of the gain values are positive excluding local times 1012 h (−4.8%), 1152 h (−0.5%), 1608 h (−0.3%), 1706 h (−15.5%) and 1722 h (−1.2%). The significant losses at 1012 h, 1706 h and 1722 h are attributed to the

Figure A 6: Comprehensive method for analysing the *PCE* of *OSCs* under different spectral irradiances considering both photonic and electrical characteristics (page 6)

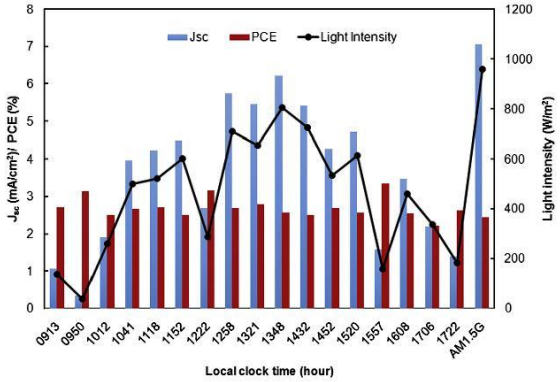

Fig. 7. Light intensity, short-circuit current density and power conversion efficiency for spectral irradiance of different local clock time from 0913 h (morning) to 1722 h (late afternoon) as well as AM1.5G for comparison.

significant red shift in the spectral irradiance at these moments. Owing to the spectral responsivity of the P3HT:PCBM solar cell, which performs best in the wavelength range 300–650 nm, the significant red shift in the spectral irradiances peaking at 650–750 nm at 1012 h, 1706 h, 1722 h has resulted in a substantial mismatch with the solar cell responsivity. In addition, we also discovered that the diffuse solar irradiance significantly favors PCE for a P3HT:PCBM solar cell at local times 0950 h, 1222 h and 1557 h with significant gains of 12.1%, 23.7% and 27.9% respectively as compared to that of AM1.5G. It can be justified by the blue shift in the spectral irradiances during a cloudy day peaking at 450–550 nm at 1222 h and 1557 h, which results in perfect matching with the highest responsivity range of a P3HT:PCBM solar cell. Based on the spectral analysis, it is recommended that organic photoabsorptive materials with responsivity covering the longer wavelength in the range of 400–900 nm will further improve the PCE under the local climate in Malaysia. This methodology can also be applied to select appropriate materials for organic solar cells under different local irradiance when optimizing the power-conversion performance.

For the second part of the study, we analyzed the annual average PCE and the annual energy yield of the P3HT:PCBM solar cell under local climate conditions. From the annual data collection, 59.7% of the annual collected local spectra are direct irradiance (the sun was unobstructed) whereas 40.3% of collected local spectra are diffuse irradiance (the sun was at least partially obstructed by clouds). Fig. 8 shows the annual average local spectra, annual average direct local spectra, and annual average diffuse local spectra from July 2015 to June 2016. From Table 2, the gain value of the annual average local spectra is 5.4% in which the diffuse component gain is 11.4% and the direct component gain is 4.8%. The annual electrical energy density yield can be computed with the following equation:

$$E_d = \text{Light intensity (kW/m}^2) \times \text{PCE (\%)} \times 365\ \text{day/year} \times 10\ \text{h/day}$$

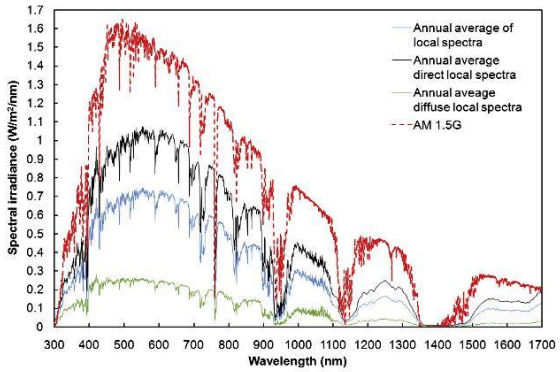

Fig. 8. Annual average local spectral irradiances from July 2015 to June 2016 for local clock time from 0800 to 1800 h at 10 min intervals per capture and comparison with AM1.5G.

Figure A 7: Comprehensive method for analysing the *PCE* of *OSCs* under different spectral irradiances considering both photonic and electrical characteristics (page 7)

Table 2
The computed values for J_{sc}, V_{oc}, FF, light intensity, PCE, and gain for annual average local spectra: total, direct and diffuse irradiances as well as AM1.5G for comparison.

	J_{sc} (mA/cm^2)	V_{oc} (V)	FF	Light intensity (W/m^2)	PCE (%)	Gain (%)
Annual average of local spectra	2.33	0.58	0.64	401	2.17	5.4
Annual average direct spectra	3.33	0.60	0.63	582	2.16	4.8
Annual average diffuse spectra	0.85	0.55	0.66	134	2.29	11.4
AM1.5G	5.14	0.61	0.62	960	2.04	–

Based on our collection of annual collected local spectra, the annual energy density yield is 31.89 kW h/m^2 (total) with 27.36 kW h/m^2 contributed by direct irradiance and 4.53 kW h/m^2 contributed by diffuse irradiance in which cosine loss is not considered in our calculation.

4. Conclusions

In this paper, we have described a comprehensive methodology to determine the PCE of organic solar cells under different spectral irradiances as opposed to conventional indicators such as APE and SMF, which rely only on optical data and shifts in J_{sc}. This is necessary for the case of organic solar cells owing to electrical properties that are impacted in ways that are different from other solar cell technologies. This method can also estimate the annual energy yield of OPVs by using local spectra data. As a case study, a P3HT:PCBM solar cell with an active area of 1 cm^2 was fabricated to study the PCE and the annual energy yield under local spectral irradiances in a city in Malaysia. Despite photocurrent output increasing proportionally with light intensity, the PCE does not change in the same way due to FF behaving in an opposite manner. In our simulation results, a spectral blue shift associated with diffuse solar irradiance was found to be in favor the P3HT:PCBM solar cell performance with significantly higher gains ranging from 23.7% to 27.9% compared to that tested under AM1.5G conditions. Through this comprehensive methodology, the annual energy density yield can also be estimated as 31.89 kW h/m^2 (total) with 27.36 kW h/m^2 contributed by direct component and 4.53 kW h/m^2 contributed by diffuse component. Lastly, the new analysis can also provide guidance on the selection of appropriate organic materials for solar cells that can perform best in a particular location in order to optimize the investment.

Acknowledgements

The authors would like to express their gratitude to Fundamental Research Grant Scheme (FRGS) by the Ministry of Higher Education with Project Number FRGS/1/2016/TK07/UTAR/01/1 for the financial support in this study. In addition, Kok-Keong Chong would like to thank the Fulbright Visiting Program for providing a fellowship for working at Princeton University.

References

[1] Pandey AK, Tyagi VV, Selvaraj JA, Rahim NA, Tyagi SK. Recent advances in solar photovoltaic systems for emerging trends and advanced applications. Renew Sustain Energy Rev 2016;53:859–84.
[2] Rohr Steffanie. 25th Anniversary article: a decade of organic/polymeric photovoltaic research. Press release; 2013. Available from: <http://www.heliatek.com/en/press/press-releases/details/heliatek-consolidates-its-technology-leadership-by-establishing-a-new-world-record-for-organic-solar-technology-with-a-cell-effi>.
[3] Gorter T, Reinders AHME. A comparison of 15 polymers for application in photovoltaic modules in PV-powered boats. Appl Energy 2012;92:286–97.
[4] Li G, Zhu R, Yang Y. Polym Solar Cells. Nat Photonics 2012;6(3):153–61.
[5] Yang X, Uddin A. Effect of thermal annealing on P3HT:PCBM bulk-heterojunction organic solar cells: a critical review. Renew Sustain Energy Rev 2014;30:324–36.
[6] Green MA, Emery K, Hishikawa Y, Warta W, Dunlop ED. Solar cell efficiency tables (version 47). Prog Photovolt: Res Appl 2016;21:827–37.
[7] Cornaro C, Andreotti A. Influence of average photon energy index on solar irradiance characteristics and outdoor performance of photovoltaic modules. Prog Photovolt Res Appl 2013;21:996–1003.
[8] Dirnberger D, Blackburn G, Müller B, Reise C. On the impact of solar spectral irradiance on the yield of different PV technologies. Sol Energy Mater Sol Cells 2015;132:431–42.
[9] Nofuentes G, García-Domingo B, Muñoz JV, Chenlo F. Analysis of the dependence of the spectral factor of some PV technologies on the solar spectrum distribution. Appl Energy 2014;113:302–9.
[10] Betts TR, Jardine CN, Gottschalg R, Infield DG, Lane K. Impact of spectral effects on the electrical parameters of multijunction amorphous silicon cells. Proceedings of 3rd world conference on photovoltaic energy conversion, vol. 2. p. 1756–9.
[11] Minemoto T, Toda M, Nagae S, Gotoh M, Nakajima A, Yamamoto K, et al. Effect of spectral irradiance distribution on the outdoor performance of amorphous Si//thin-film crystalline Si stacked photovoltaic modules. Sol Energy Mater Sol Cells 2007;91(2–3):120–2.
[12] Minemoto T, Nagae S, Takakura H. Impact of spectral irradiance distribution and temperature on the outdoor performance of amorphous Si photovoltaic modules. Sol Energy Mater Sol Cells 2007;91(10):919–23.
[13] Minemoto T, Nakada Y, Takahashi H, Takakura H. Uniqueness verification of solar spectrum index of average photon energy for evaluating outdoor performance of photovoltaic modules. Sol Energy 2009;83(8):1294–9.
[14] Ishii T, Otani K, Takashima T. Effects of solar spectrum and module temperature on outdoor performance of photovoltaic modules in round-robin measurement in Japan. Prog Photovolt: Res Appl 2011;19:141–8.
[15] Sirisamphanwong C, Ketjoy N. Impact of spectral irradiance distribution on the outdoor performance of photovoltaic system under Thai climatic conditions. Renew Energy 2012;38(1):69–74.
[16] Dirnberger D, Muller B, Reise C. On the uncertainty of energetic impact on the yield of different PV technologies due to varying spectral irradiance. Sol Energy 2015;111:82–96.
[17] Jardine C, Betts T, Gottschlg R, Infield DG, Lane K. Influence of spectral effects on the performance of multijunction amorphous silicon cells. 17th Eur photovolt sol energy conf, vol. 44. p. 2–5.
[18] Moreno-Sáez R, Mora-López L. Modelling the distribution of solar spectral irradiance using data mining techniques. Environ Model Softw 2014;53:163–72.
[19] Senthilarasu S, Fernández EF, Almonacid F, Mallick TK. Effects of spectral coupling on perovskite solar cells under diverse climatic conditions. Sol Energy Mater Sol Cells 2015;133:92–8.
[20] Foertig A, Rauh J, Dyakonov V, Deibel C. Shockley equation parameters of P3HT:PCBM solar cells determined by transient techniques. Phys Rev B 2012;86:115302.
[21] Koster LJA, Mihailetchi VD, Ramaker R, Blom PWM. Light intensity dependence of open-circuit voltage of polymer:fullerene solar cells. Appl Phys Lett 2005;86:123509.
[22] Rand BP, Burk DP, Forrest SR. Offset energies at organic semiconductor heterojunctions and their influence on the open-circuit voltage of thin-film solar cells. Phys Rev B 2007;75:115327.
[23] Giebink NC, Wiederrecht GP, Wasielewski MR, Forrest SR. Ideal diode equation for organic heterojunctions. I. Derivation and application. Phys Rev B 2010;82:155305.
[24] Jin H, Armin A, Hambsch M, Lin Q, Burn PL, Meredith P. Bulk heterojunction thickness uniformity – a limiting factor in large area organic solar cells? Phys Status Solidi 2015;212(10):2246–54.
[25] Yoo S, Domercq B, Kippelen B. Intensity-dependent equivalent circuit parameters of organic solar cells based on pentacene and C_{60}. J Appl Phys 2005;97(10):103706.
[26] Wu L, Zang H, Hsiao Y-C, Zhang X, Hu B. Origin of the fill factor loss in bulk-heterojunction organic solar cells. Appl Phys Lett 2014;104(15):153903.
[27] Jin H, Armin A, Hambsch M, Lin Q, Burn PL, Meredith P. Bulk heterojunction thickness uniformity – a limiting factor in large area organic solar cells? Phys Status Solidi A 2015:1–9. http://dx.doi.org/10.1002/pssa.201532353.

Figure A 8: Comprehensive method for analysing the *PCE* of *OSCs* under different spectral irradiances considering both photonic and electrical characteristics (page 8)